Supplementary Information (SI) for RSC Sustainability.

Supplementary information for

Surfactant-free gold nanoparticles synthesized in alkaline water-ethanol mixtures: leveraging lower grade chemicals for size control of active nanocatalysts

Frederik Jæger,[a,†] Albert Abildtrup Pedersen,[a,†] Peter Stensgaard Wacherhausen,[a,†] Aleksandra Smolska,[a,†] Jonathan Quinson [a,*]

a) Nanomaterials Engineering for Sustainable Technologies (NEST) group,
Biological and Chemical Engineering Department,
Aarhus University, 40 Åbogade, 8200 Aarhus, Denmark

† Equally contributing authors

* corresponding author: jquinson@bce.au.dk

1 - Materials and methods

Materials and Methods

Chemicals

All chemicals were used as received: $HAuCl_4{\cdot}3H_2O$ (99%, BLD Pharmatech, referred to as $HAuCl_4$ -); $HAuCl_4{\cdot}3H_2O$ (≥99.7%, MP Biomedical, referred to as $HAuCl_4$ +); NaOH (Reag. Ph. Eur., VWR); ultrapure water (mQ, Milli-Q, Millipore, resistivity of >18.2 MΩ•cm); de-ionized water (DI, 21.5 µS cm^{-1}); HCl (puriss. ACS reagent, reag. ISO, Reag. Ph. Eur. fuming, $\geq$ 37%, Sigma Aldrich); HNO_3 (puriss $\geq$ 65%, Sigma Aldrich); Ethanol ($E_{70\%}$, Ethanol 70% (v/v), TechniSolv®, VWR); Ethanol ($E_{99.8\%}$, Ethanol absolute, ≥99.8%, AnalaR NORMAPUR® ACS, Reag. Ph. Eur. analyse reagens, VWR); glycerol (bi-distilled 99.5%, VWR); ethylene glycol (EMSURE®, Reag. Ph. Eur. Reag. USP, Supelco®); $NaBH_4$ (ReagentPlus®, 99%, Sigma-Aldrich), 4-nitrophenol (4-NP, ReagentPlus®, ≥99%, Sigma-Aldrich).

Extra caution was taken so that none of the chemicals were in contact with metal (e.g. metallic spatulas were not used and plastic spatulas were preferred). **Dispose of chemicals following local rules. Pay attention to HCl, HNO_3 and 4-NP based wastes**.

Au NP synthesis

The synthesis follows the optimal parameters suggested in previous studies.[1] The stock solution of NaOH was at 50 mM in mQ water, stored in Nalgen flasks.[2] The stock solution of $HAuCl_4$ was at 50 mM in mQ, kept in a borosilicate glass vial in a fridge at ca. 5 °C and covered in aluminum when left at room temperature (RT) to avoid any light-induced side-reactions. The final concentrations before taking into account volume contraction were 80 v.% water (with different ratios of mQ and DI water, and in the following the effect of the total amount of DI water in v.% is explored), 20 v.% ethanol, 2 mM NaOH and 0.5 mM $HAuCl_4$, for a total volume of 2 mL (before taking into account volume contraction).[1] A NaOH/Au molar ratio of 4 was previously established as an optimal value in light of the equation of the reduction process.[1] The overall synthesis process is schematized in **Figure S1**.

The reaction was performed in disposable 1 cm wide rectangular polystyrene (PS) UV-vis cuvettes (340-900 nm, VWR, 634-0675), simply de-dusted with a gentle flow of compressed air before being used. The magnets used for stirring (PTFE cylindrical stirrer bar, 8 x 3 mm, VWR, 442-4520) were cleaned with *aqua regia* (4:1, v:v, HCl:HNO_3; ***to be handled and disposed of with care following the related safety procedures in place in the laboratory***), washed with copious amount of water, and de-dusted prior to use.[3] The chemicals from the different stock solutions were added in the order: water < base < alcohol < $HAuCl_4$.[1] $HAuCl_4$ was therefore added last,[1] under stirring (500 rpm) in a photo-box (Puluz LED portable Photo Studio, PU5060EU, 60 cm x 60 cm x 60 cm, 60 W) to control light environment for the synthesis.[1,4] The samples were capped (Kartell™ Dispolab™ push-in polyethylene – PE – stoppers) and left to react for two hours in the photo-box with stirring. The capping is aimed at minimizing cross contamination and possible ethanol evaporation, although in we observed that the experiments can be performed uncapped for two hours without much influence on the final volume of the samples, which suggest minimal evaporation from the ethanol-water mixture. The samples were then left for 1 day at RT and ambient light without stirring before the magnets were removed and the samples closed again, sealed with Parafilm®. The samples were then further stored in a drawer at RT (not in a fridge, to save further energy), unless otherwise specified. Note that RT was between 20 and 25 °C and we observed in previous study that temperatures below 30-40 °C does not have a strong influence on the outcome of the synthesis.[1,5]

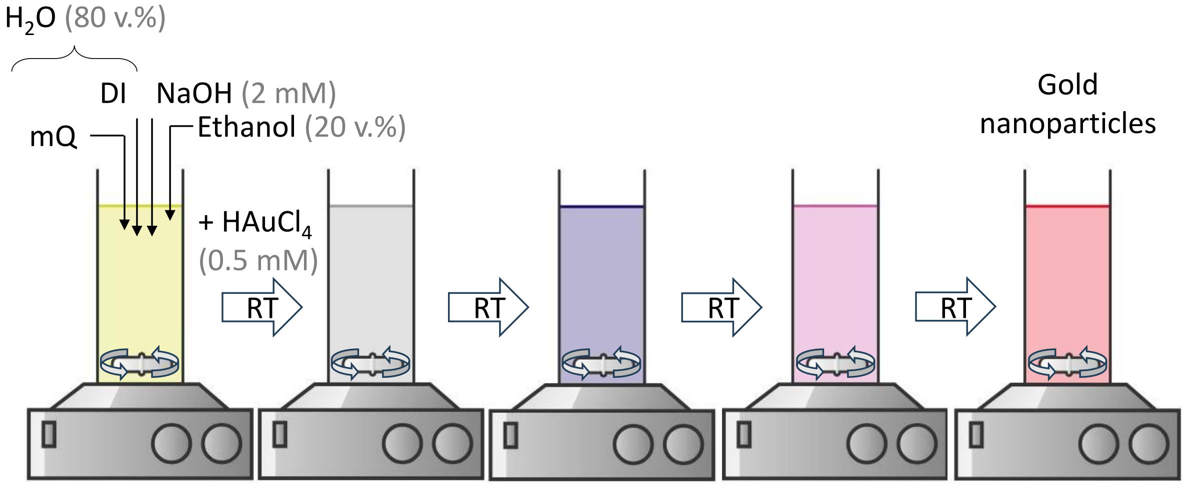

Figure S1. Illustrative scheme of the synthesis that consists in mixing mQ, DI (where the amount of mQ+DI is 80 v.%), NaOH and ethanol (where the amount of ethanol is 20 v.%) to which $HAuCl_4$ is added last under stirring. The values indicated in grey are the final concentrations. RT stands for room temperature. Diagram(s) created with Chemix (2025). Retrieved from https://chemix.org and adapted.

For a controlled experiment, gold (Au) nanoparticles (NPs) ca. 10 nm were prepared by adding a freshly prepared solution of $NaBH_4$ to $HAuCl_4$ in mQ.[6] The $HAuCl_4$ solution was prepared from a stock solution at 50 mM, so that the final volume of solution was 3 mL, the final concentration of $HAuCl_4$ was 0.5 mM and the $NaBH_4$/Au molar ratio was 8 or 9. The experiment was performed in the same UV-vis cuvette as above and under stirring. The solution turns red immediately after addition of $NaBH_4$.

Notes on Sustainable Chemistry

The ability to perform the synthesis at RT due to the redox properties of the gold precursor, with minimal equipment and using benign chemicals (e.g. avoiding surfactants typically derived from fossil fuels, or plant extracts requiring extraction in organic solvents[1]) complies with the principle of *Green Chemistry* and *Sustainable practices in academic research*.[7-10]

Although the use of disposable UV-vis cuvettes generates plastic waste, the ability to perform the synthesis in small volume minimizes waste and limits the use of *aqua regia* to clean the magnets only, and not the all (larger) glassware as opposed to other synthetic strategies.[3] It also facilitates storage.

The use of 0.5 mM $HAuCl_4$ is on the high end of concentrations reported for Au NPs synthesis[3] and is relevant to explore to minimize the volume of chemicals used upon scale up.

Furthermore, it is common to prefer high purity chemicals, e.g. $HAuCl_4$ with purity ≥ 99.9%.[11,12] In view of scale up, we here prefer a lower grade and cheaper chemical (99%) that is also suitable to obtain the NPs, as detailed below.

The synthesis can be performed without stirring and in theory at ambient light, which reduces even further the energy cost. However, more reproducible results are obtained using stirring and controlled light environment obtained here using a simple photobox.[4,5]

The stock solutions and colloidal dispersions were stored at RT to avoid the use of energy consuming fridges. Only the stock solutions of 4-NP were stored in a fridge.

Although this is beyond the scope of this study, the recycling of the Au atoms in a natural further step in this research area.[13]

Characterization

A focus for this study is given to the properties retrieved from UV-vis measurements.[1] This is because UV-vis spectra are informative when it comes to Au NP characteristics, and because to develop more sustainable research,[7] it will not be realistic to use all characterization methods reported for Au NPs.[14,15] Complementary characterization has been reported in previous work such as XRD, XPS, HR-TEM, X-ray total scattering with pair distribution function analysis and zeta-potential measurements.[1]

UV-vis characterization

A Shimadzu UV-1800 UV/Visible scanning spectrophotometer was used and the spectra recorded between 290 and 800 nm. The solutions were measured as-prepared in the 1 cm width squared shape UV-vis cuvettes used for the synthesis as detailed in the section *Au NPs synthesis*. As baseline, a solution of 20 v.% of the ethanol and 80 v.% mQ water were used (no base, no DI water).

The Mie theory correlates various variables to the optical properties of Au NPs.[16-18] Note that UV-vis spectra of Au NPs results from a complex interplay between the properties of gold, nanoscale effects (such as size and shape) and interaction with the solvents and/or interactions between NPs and precursor.[19] Nevertheless, due to their plasmonic properties (surface plasmon resonance, spr), several parameters descriptive of the Au NPs can be retrieved, λ_{spr}, A_{spr}/A_{450}, A_{380}/A_{800}, A_{650}/A_{spr} and A_{400}, all defined, detailed and summarized in **Table S1**.

All samples were typically measured the day after synthesis (at least within 2 days after synthesis). For stability over time, samples were measured several days up to a month after the synthesis, as indicated.

STEM characterization

STEM micrographs were recorded on an FEI Talos F200X operated at 200 kV, equipped with a high-angle annular dark-field (HAADF) detector. The as-prepared colloidal dispersions were dropped on Copper TEM grids (Sigma-Aldrich), placed on an absorbing filter paper, and the solvent was left to evaporate. The samples were characterized by imaging at least 3 randomly selected areas at 3 different magnifications. Typically, at least 100 NPs were used to estimate the size (diameter) of the NPs (N values reported below correspond to the number of NPs counted). The size analysis was performed using the ImageJ software.

pH measurements

pH is an important parameter to control Au NP synthesis.[11] Three main reasons refrained us to report in detail pH values at this stage: (i) we here use mixtures of water and alcohol and therefore pH is not really defined (pH is defined for a purely aqueous medium); (ii) we observed that using a pH probe destabilized the colloids; (iii) using a pH-strip is possible but the red colour of the colloids can complicate the reading. Further investigation is being performed to clarify the effect and importance of pH in the reaction.

Based on our first estimations using pH probe (Sigma-Aldrich® micro pH combination electrode), the initial pH before adding $HAuCl_4$ is around 9-10, it drops right after $HAuCl_4$ is added and typically stabilizes at a value around 4-5, in agreement with the equation of the reaction.[1]

Conductivity measurements

Conductivity measurements were carried out using a CDM210 conductivity meter (Radiometer Analytical) equipped with a conductivity cell (cell constant of 0.985 cm^{-1}). Four sets of aqueous mixtures (for a total volume 50 mL per sample) were prepared using mQ DI absolute ethanol and/or NaOH: (**1**) DI and mQ water in different ratios (total amount of water is 100%), (**2**) 20 v.% of ethanol and 80 v.% water, where the later amount of water is a mixture of mQ and DI water in different ratios (in this case the ratio indicated are the ratios of DI water in the 80 v.% of total water), (**3**) the same solutions as (1) but with 0.1 mL of 1 M NaOH added, giving a final NaOH concentration of 2 mM. The small addition volume did not significantly affect the water ratio, so this effect can be neglected. (**4**) the same as (2) but with 0.1 mL of 1 M NaOH added, giving a final NaOH concentration of 2 mM (in this case the ratio indicated are the ratios of DI water in the 80 v.% of total water). The small addition volume did not significantly affect the water ratio, so this effect can be neglected. Additionally, 100% DI water was measured on different days and/or from different sources to assess variability in the DI supply. All measurements were performed at room temperature (25 ± 2°C) in triplicate. Solutions were freshly prepared, thoroughly mixed and measured without stirring, after allowing the conductivity meter reading to stabilize.

4-nitrophenol reduction

The catalytic activity of the Au NPs was evaluated for the 4-nitrophenol (4-NP) reduction to 4-aminophenol (4-AP) at RT. The following stock solutions were used: 1 mM 4-NP in mQ water, 100 mM $NaBH_4$ in mQ water and 0.5 mM as prepared Au NPs (Au equivalent). Fresh stock solutions of $NaBH_4$ were prepared before every reaction. The Au NPs were prepared as described in the *Au NP synthesis* section. All solutions were purged with nitrogen (99.9%), excluding Au NPs due to the small volume of solution used (typically 10 µL), before the reaction to remove dissolved oxygen.[20] The reaction was performed in a total volume of 2 mL with final concentrations of 0.05 mM 4-NP, 5 mM $NaBH_4$ ($NaBH_4$/4-NP molar ratio of 100) and 0.0025 mM of Au NPs (Au equivalent, Au/4-NP molar ratio of 5%), unless otherwise specified.

To comply with the principle of sustainability in the laboratory,[7] we aimed to minimize the volume of 4-NP to use and the kinetics studies were performed in UV-vis cuvettes directly placed in a Go Direct® UV-vis spectrophotometer with a fixed scan range of 220 nm to 850 nm. It takes only ca. 1-2 seconds to acquire the whole range. The background was a solution of mQ. Spectra were recorded every 40 to 180 seconds with the first spectra 20 seconds after Au NPs were added. The reactions were performed directly in disposable 1 cm wide rectangular polystyrene (PS) UV-vis cuvettes (340-900 nm, VWR, 634-0675). To ensure uniform conditions, the reaction was magnetically stirred at 550 rpm and performed under LED light in a photo-box (Puluz LED portable Photo Studio, PU5060EU, 60 cm x 60 cm x 60 cm, 60 W). The cuvette was then sealed with a dedicated cap immediately after the addition of the reactants. The reaction was initiated by adding the Au NPs to the mixture of $NaBH_4$ and 4-NP.

The progress of the 4-NP reduction to 4-AP was monitored following the time-related decrease of the characteristic absorption peak of the nitrophenolate anion at 400 nm. At the same time, a weaker absorption peak increases at around 300 nm, which corresponds to the formation of 4-AP.[21] A pseudo-first-order kinetics was assumed, given the large excess of $NaBH_4$, relative to 4-NP.[6] Data obtained from the UV-Vis measurements were used to fit the kinetic model and evaluate rate constants and turnover frequency, as detailed elsewhere.[22]

Note that due to the relatively poor resolution of the equipment to compromise with a fast acquisition time, the small volume of solution used and the fact that measurements were performed under stirring, some fluctuations similar to those observed in **Figure S15c** and **Figure S18c** were observed. Those fluctuations are attributed to the stirring and/or gas bubbles formation on the path of the UV light, punctually altering the measurements. Rather than removing the related data points we prefer to report all data. The metrics retrieved and the related fits were performed without taking into account those outliers.

It is assumed that the concentration of 4-NP in presence of $NaBH_4$ (i.e. 4-nitrophenolate) at a given time t, is given by $C_t=C_0e^{-k_{app}t}$, where C_0 is the initial concentration of 4-NP / 4-nitrophenolate at t = 0 s. Since there is a large excess of $NaBH_4$ the kinetic constant k_{app} is not expected to depend on the concentration of $NaBH_4$. Taking into account the Beer-Lambert's law that establishes that the absorbance of a species is proportional to its concentration in solution the relationship can be expressed as $A_t=A_0e^{-k_{app}t}$, where A_t is the absorbance at 400 nm at a given time and A_0 the absorbance at t = 0 s. Thus, $-\ln(A_t/A_0)=k_{app}.t$ should be a linear function of time.[22] The turnover frequency was estimated as: $\mathrm{TOF} = \frac{\mathrm{C_0}\ (mol)}{\mathrm{n_{Au}}\ (mol)} \frac{\mathrm{Conversion\ (\%)/100}}{\mathrm{t}\ (h)}$, where n_{Au} is the nominal amount of Au in moles, t is the time required to reach a given conversion estimated from UV-vis.

The TOFs were estimated in different ways. TOF_t corresponds to the TOF estimated after a given reaction time as indicated in **Table S5**. $TOF_{t\text{-}A400}$ corresponds to the TOF_t normalized by the A_{400} value retrieved from UV_{vis} (absorbance at 400 nm that is proportional to the amount of Au^0 and therefore NPs in the dispersions[16]). $TOF_{\%}$ corresponds to the TOF estimated considering the maximum conversion reached for the total duration of the experiments as indicated in **Table S5**. $TOF_{\%\text{-}A400}$ corresponds to the $TOF_{\%}$ normalized by the A_{400} value.

2- UV-vis metrics

Table S1. Parameters retrieved from UV-vis spectroscopy. Note that the relationships summarized typically assume spherical NPs within a given size range and are general (not absolute) trends.

Parameter	**Definition**	**Interpretation in first approximation**	**Ref.**
λ_{spr} nm	position of the localised surface plasmon resonance	$\lambda_{spr} \nearrow \leftrightarrow$ NP sizes $\nearrow$	18
A_{spr}/A_{450} -	ratio of the absorbances at λ_{pr} and 450 nm	$A_{spr}/A_{450} \nearrow \leftrightarrow$ NP sizes $\nearrow$	18
A_{400} a.u.	absorbance at 400 nm (typically normalised)	$A_{400} \nearrow \leftrightarrow$ relative yield $\nearrow$	16
A_{380}/A_{800} -	ratio of the absorbances at 300 nm and 800 nm	$A_{380}/A_{800} \nearrow$: higher stability	23
A_{650}/A_{spr} -	ratio of the absorbances at 650 nm and λ_{spr}	$A_{650}/A_{spr} \nearrow$: higher aggregation	24,25

3- Precursor and NaOH/Au molar ratio

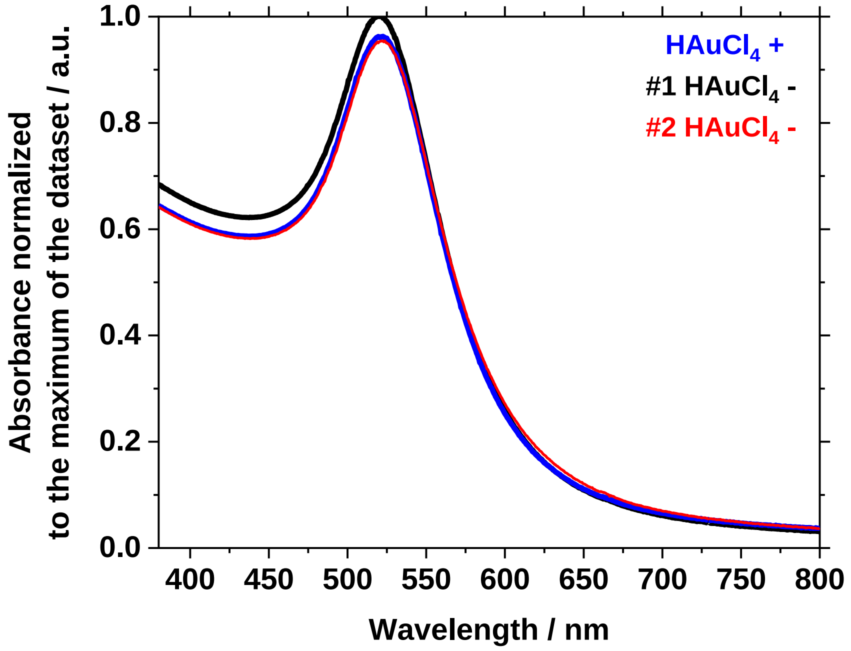

Figure S2. UV-vis spectra of Au NP colloidal dispersions obtained with 80 v.% mQ water, 20 v.% ethanol, 0.5 mM $HAuCl_4$ and a NaOH/Au molar ratio of 4.0. The samples were prepared from different precursor grade for $HAuCl_4$ ($HAuCl_4$ + and $HAuCl_4$ -, see experimental section) and two different batches of stock solutions for the lower grade precursor (#1 and #2, prepared from the same stock of powder $HAuCl_4$ -). High purity absolute ethanol ($E_{99.8\%}$) was used as stock solution of ethanol for all experiments.

The results in **Figure S2** show that the characteristic UV-vis spectra of Au NPs are obtained in all cases and therefore the use of lower grade and cheaper $HAuCl_4$ does not prevent the formation of the Au NPs. The use of higher purity $HAuCl_4$ (≥99.9%) preferred in previous studies,[1,11] is not a requirement for a successful synthesis. The results also illustrate the potential variability in the preparation of the stock solution of $HAuCl_4$ which can at least partially explain the slightly higher absorbance at 400 nm. The same stock solution #2 was used for all results in this study.

a)

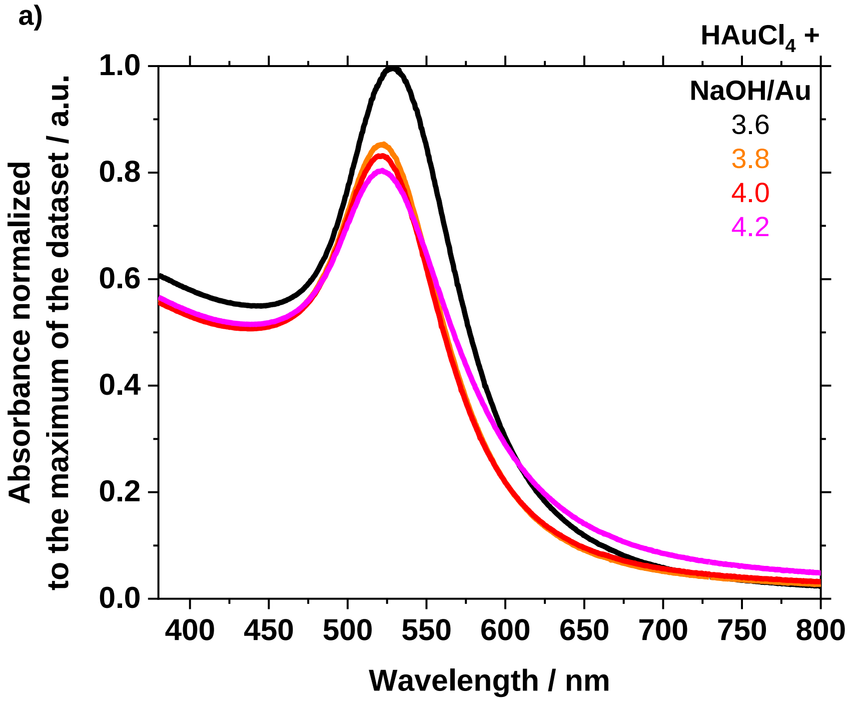
HAuCl$_4$ +
NaOH/Au
3.6
3.8
4.0
4.2
Absorbance normalized to the maximum of the dataset / a.u.
0.0
0.2
0.4
0.6
0.8
1.0
Wavelength / nm
400
450
500
550
600
650
700
750
800

b)

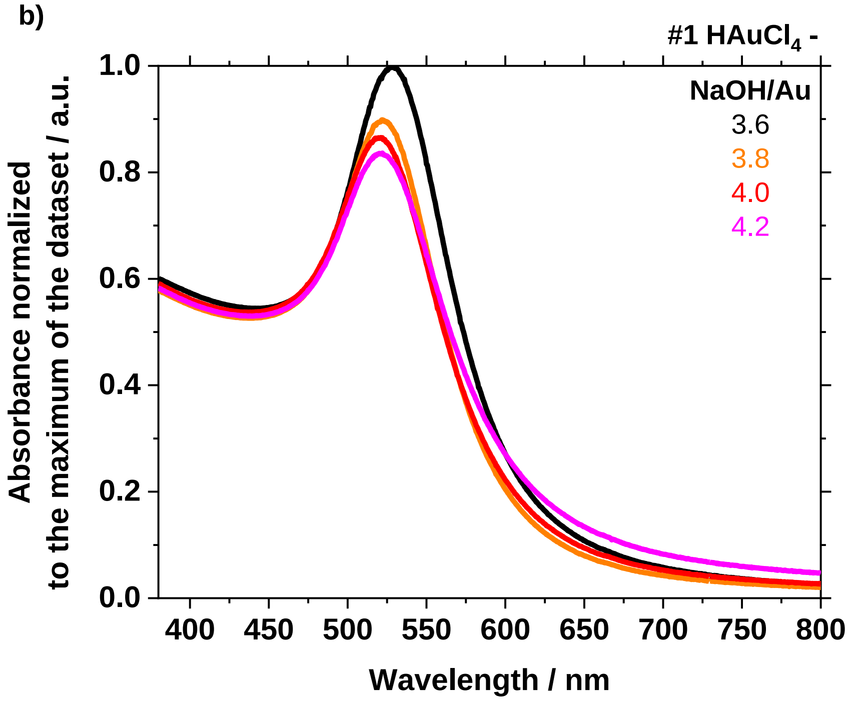
#1 HAuCl$_4$ -
NaOH/Au
3.6
3.8
4.0
4.2
Absorbance normalized to the maximum of the dataset / a.u.
0.0
0.2
0.4
0.6
0.8
1.0
Wavelength / nm
400
450
500
550
600
650
700
750
800

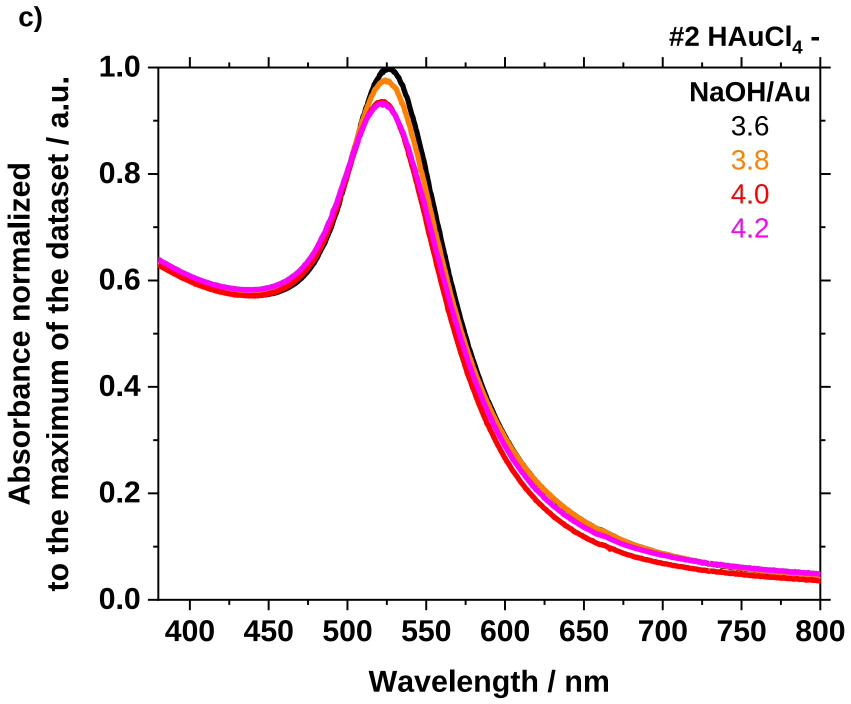

Figure S3. UV-vis spectra of Au NP colloidal dispersion obtained with 80 v.% mQ water, 20 v.% ethanol, 0.5 mM $HAuCl_4$ and (a-c) different NaOH/Au molar ratios, as indicated and for different $HAuCl_4$ precursor, as defined in Figure S1. High purity absolute ethanol ($E_{99.8\%}$) was used as stock solution of ethanol for all experiments.

From the results in **Figure S3**, an optimal value to obtain small size Au NPs (lower λ_{spr}) is a NaOH/Au molar ratio of 4.0 given that the benefits to use higher ratio (requiring more chemicals) is not pronounced (e.g. for 4.2). The two spectra for NaOH/Au molar ratio of 4.0 and 4.2 almost overlap although the spectra recorded for a NaOH/Au molar ratio of 4.2 (e.g. in **Figure S3c**) shows higher absorbance at higher wavelengths (indicative of larger and/or less stable NPs).

The results also show that some degree of size control (different λ_{spr} values) is possible by controlling the NaOH/Au molar ratio but this approach is not necessarily simple to reproduce. Furthermore, and although the concentrations of base are here relatively low, the strategy of tuning the NaOH/Au molar ratio requires to handle a relatively hazardous chemical. It would be beneficial to avoid using higher concentrations of base to achieve size control. As for lower concentration of base (e.g. 3.6) it is observed that the results are challenging to reproduce and too low values below 4.0 might lead to cases where sub-stoichiometric amounts of base are used.[1]

4-UV-vis analysis

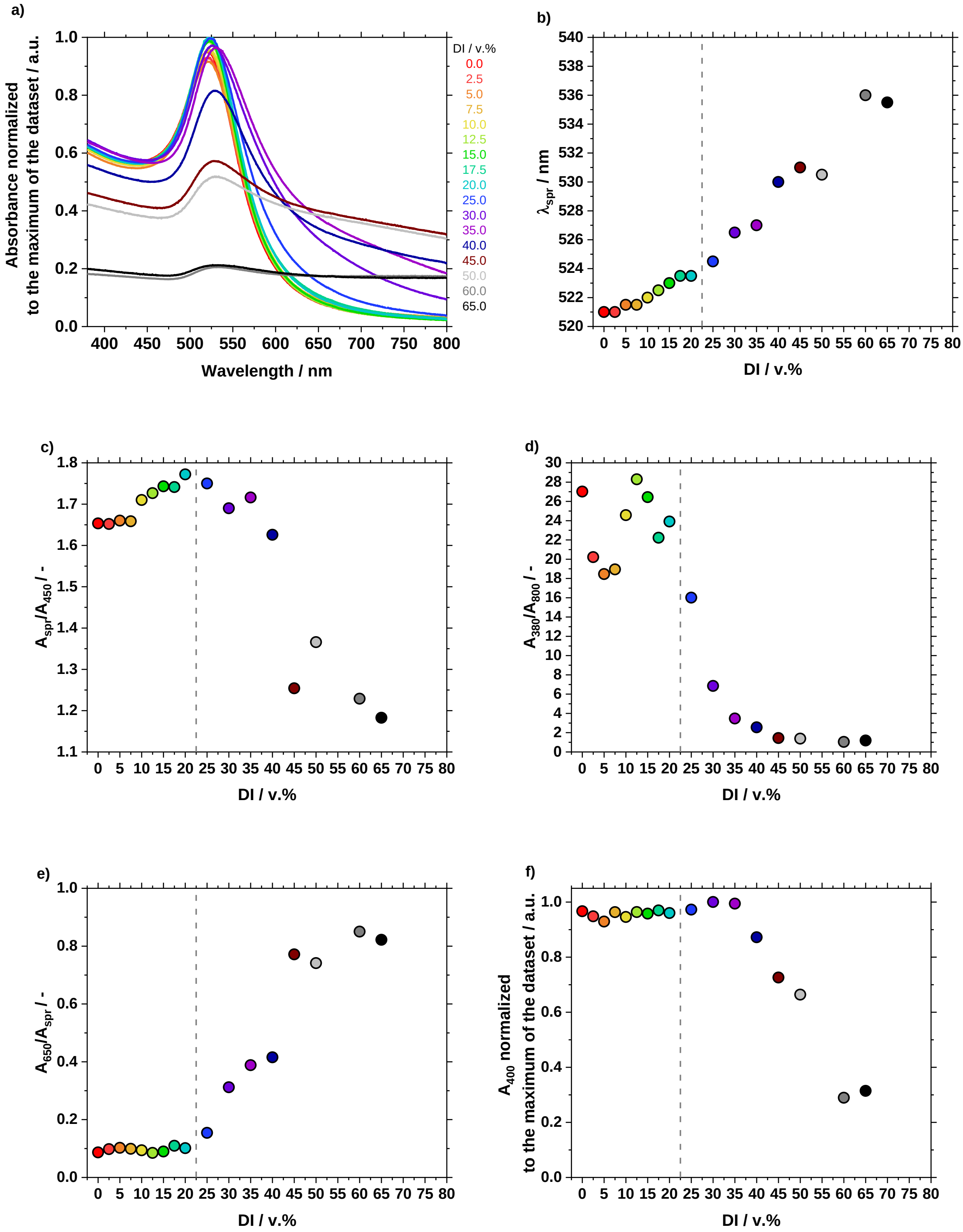

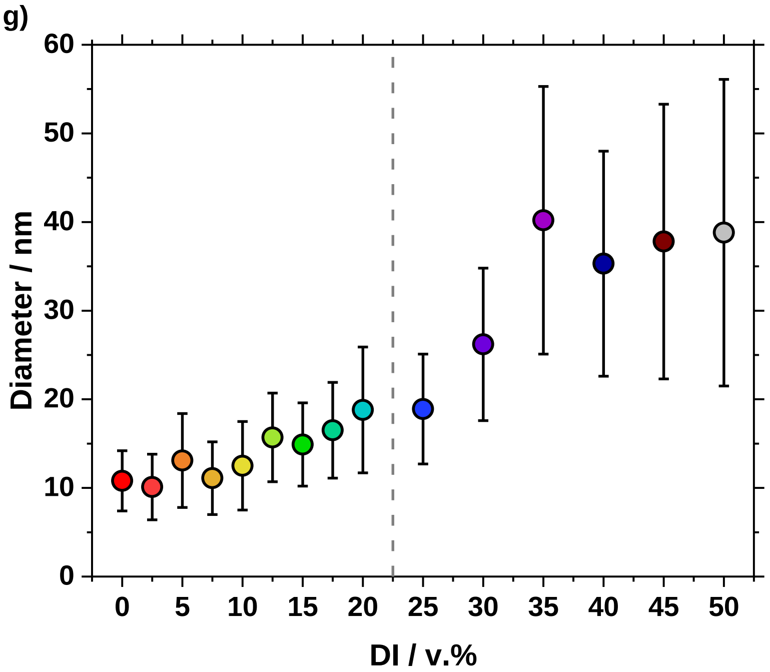

Figure S4. (a) UV-vis spectra of Au NP dispersions obtained using different v.% of DI, as indicated. Figure S4a is the same figure as **Figure 1b** from the main manuscript, reported here to facilitate the comparison with the reproduced experiments detailed below. (b-f) Various metrics retrieved from UV-vis as a function of DI water content: (b) λ_{spr}, (c) A_{spr}/A_{450}, (d) A_{380}/A_{800}, (e) A_{650}/A_{spr}, and (f) A_{400} (normalized). (g) Diameter retrieved from STEM analysis as a function of DI content. **Figure S4g** is the same figure and **Figure 1c** from the main manuscript, reproduced here to facilitate the comparison with the reproduced experiments detailed below. The dotted vertical line corresponds to the value of 22.5 v.% DI water which indicates the point where the NPs tend to stop being spherical at higher DI contents, as detailed in **Figure S5**. Low purity ethanol ($E_{70\%}$) was used as the stock solution of ethanol for all experiments at a final content of 20 v.%, for a total of 80 v.% water (DI+mQ). 0.5 mM $HAuCl_4$ and 2 mM NaOH were used in all cases.

5-STEM analysis

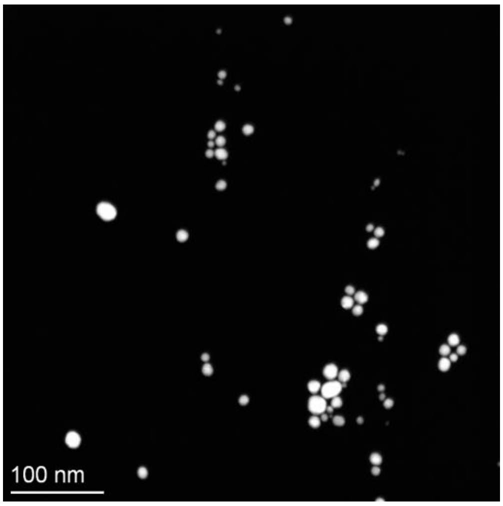

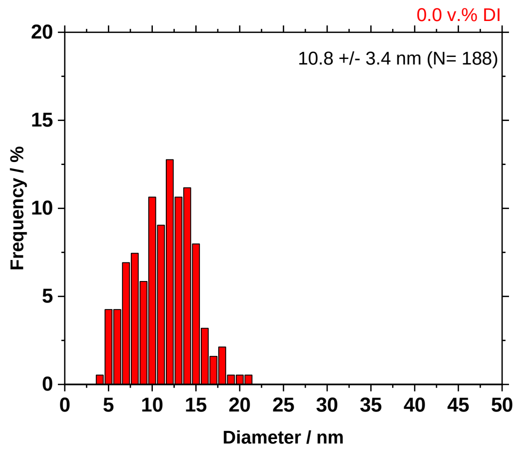

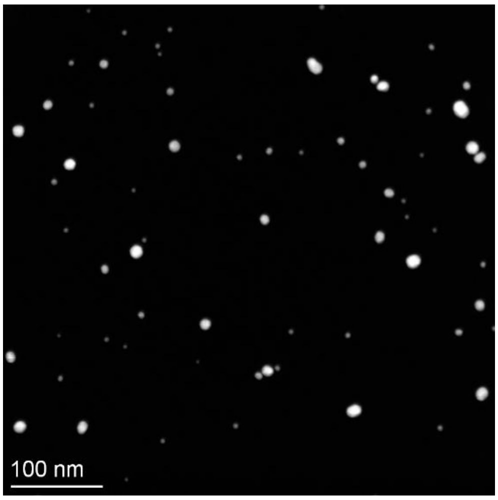

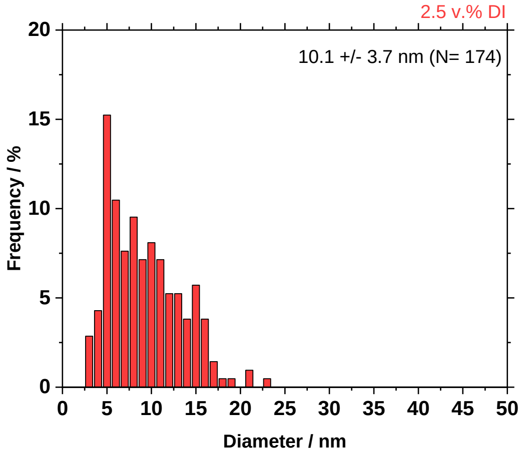

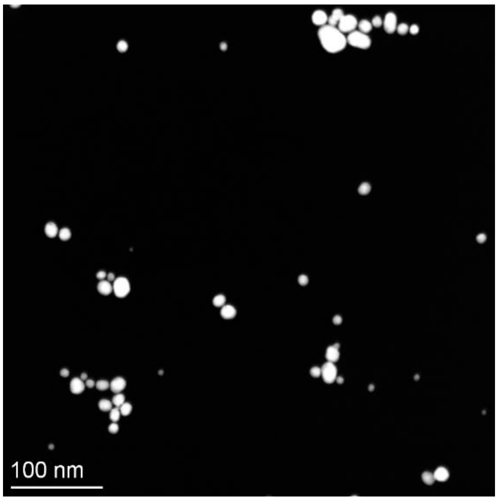

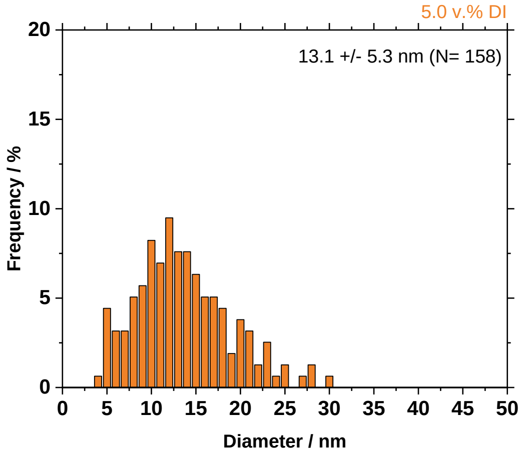

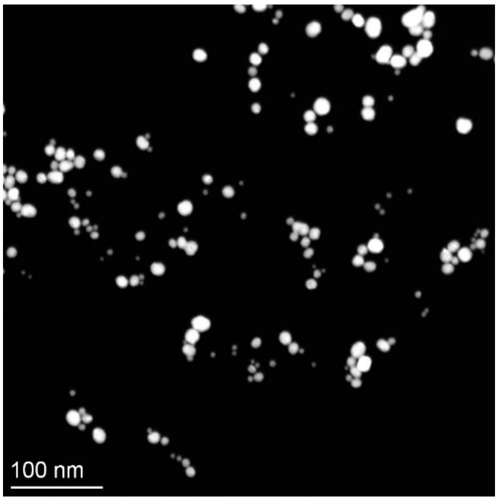
100 nm

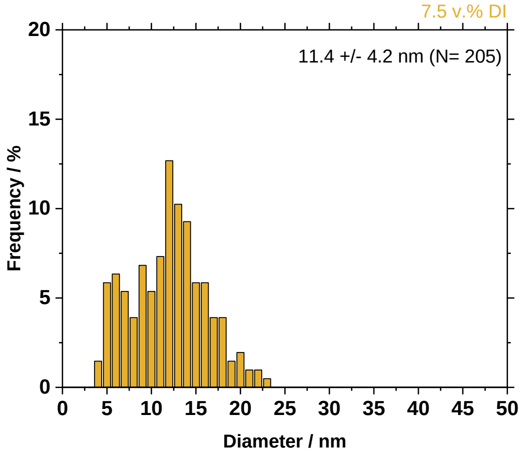
7.5 v.% DI
11.4 +/- 4.2 nm (N= 205)
Frequency / %
0
5
10
15
20
Diameter / nm
0
5
10
15
20
25
30
35
40
45
50

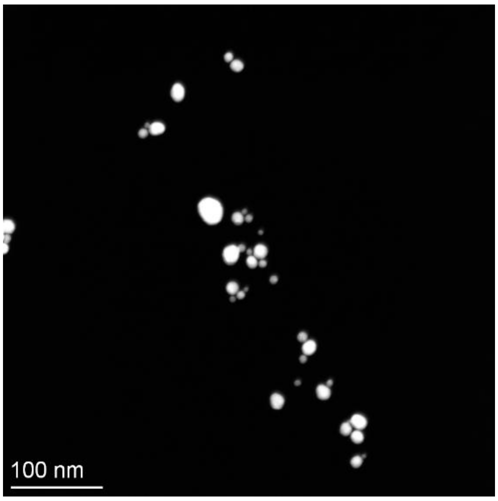
100 nm

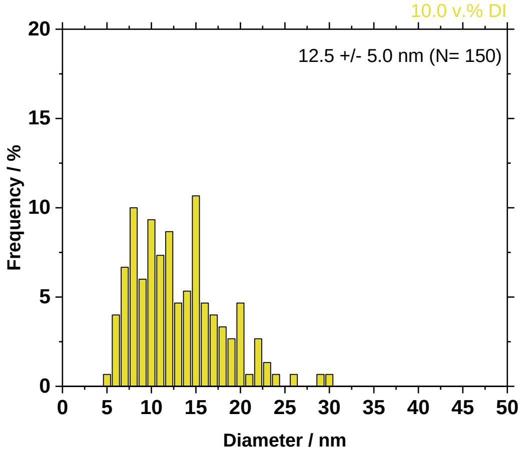
10.0 v.% DI
12.5 +/- 5.0 nm (N= 150)
Frequency / %
0
5
10
15
20
Diameter / nm
0
5
10
15
20
25
30
35
40
45
50

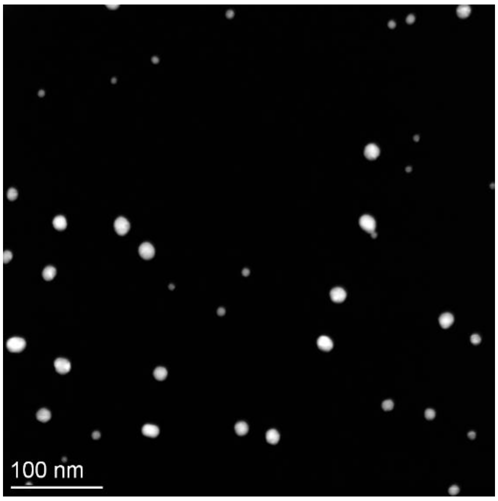
100 nm

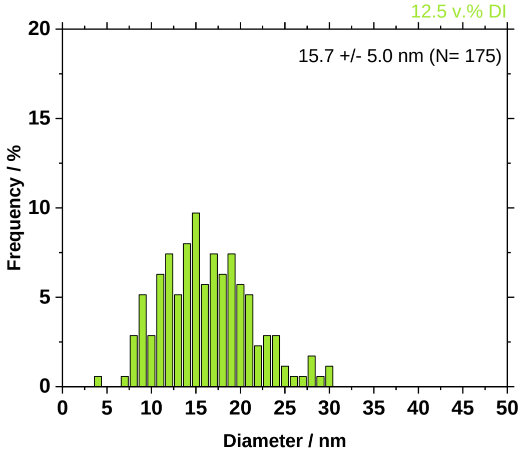
12.5 v.% DI
15.7 +/- 5.0 nm (N= 175)
Frequency / %
0
5
10
15
20
Diameter / nm
0
5
10
15
20
25
30
35
40
45
50

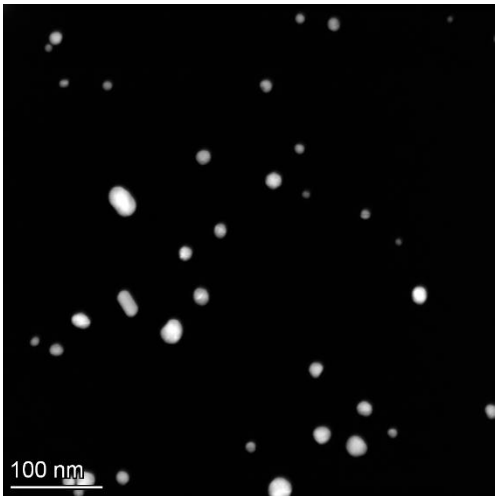
100 nm

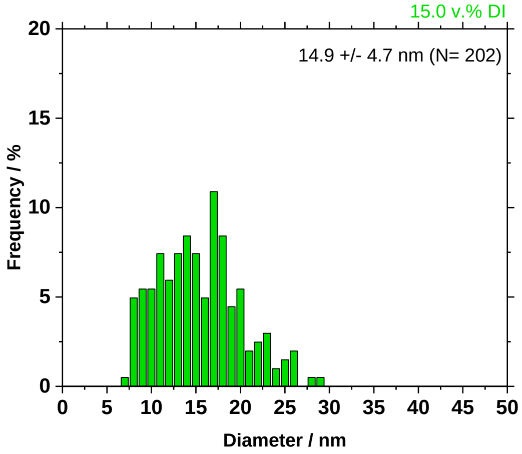
15.0 v.% DI
14.9 +/- 4.7 nm (N= 202)
Frequency / %
0
5
10
15
20
0
5
10
15
20
25
30
35
40
45
50
Diameter / nm

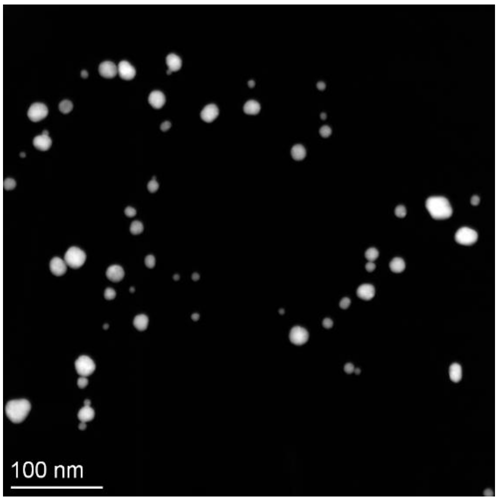
100 nm

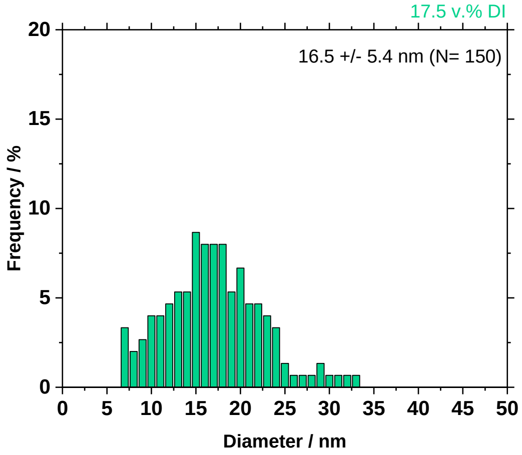
17.5 v.% DI
16.5 +/- 5.4 nm (N= 150)
Frequency / %
0
5
10
15
20
0
5
10
15
20
25
30
35
40
45
50
Diameter / nm

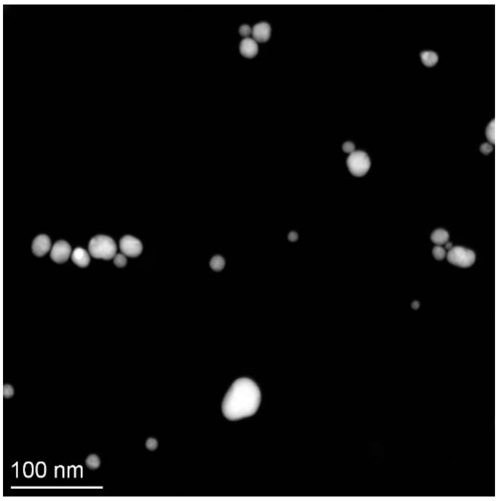
100 nm

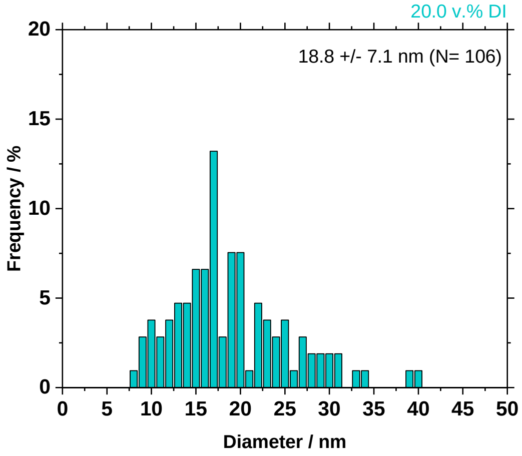
20.0 v.% DI
18.8 +/- 7.1 nm (N= 106)
Frequency / %
0
5
10
15
20
0
5
10
15
20
25
30
35
40
45
50
Diameter / nm

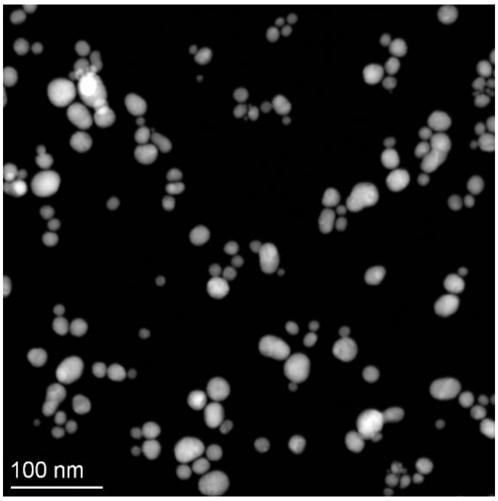
100 nm

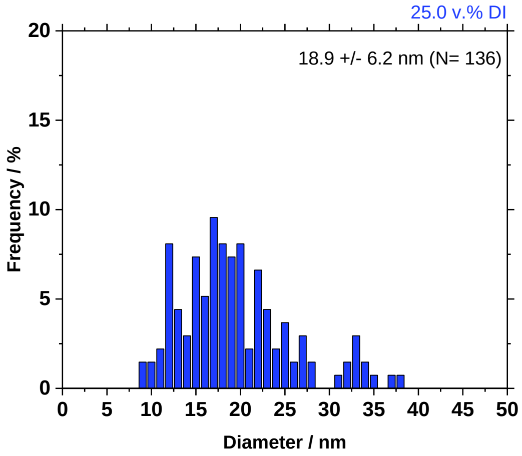
25.0 v.% DI
18.9 +/- 6.2 nm (N= 136)
Frequency / %
Diameter / nm
0
5
10
15
20
25
30
35
40
45
50

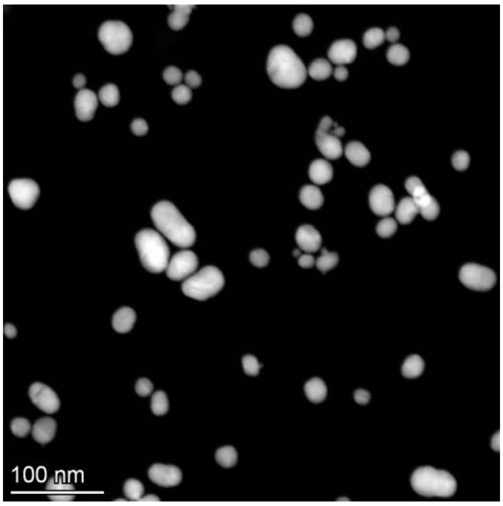
100 nm

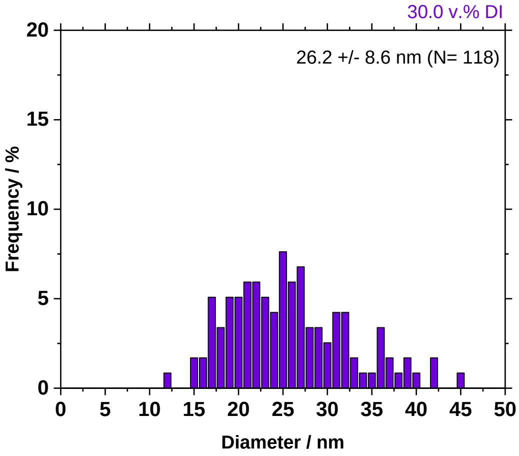
30.0 v.% DI
26.2 +/- 8.6 nm (N= 118)
Frequency / %
Diameter / nm
0
5
10
15
20
25
30
35
40
45
50

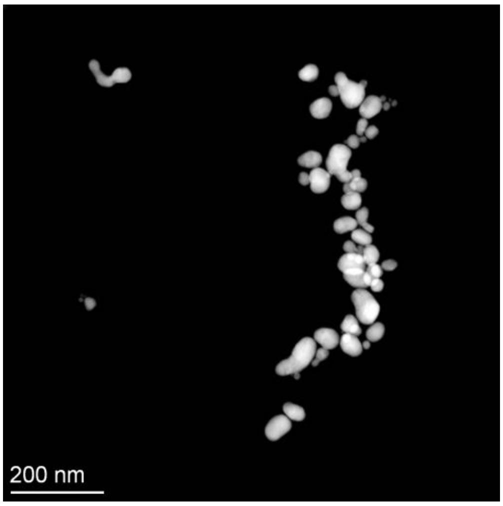
200 nm

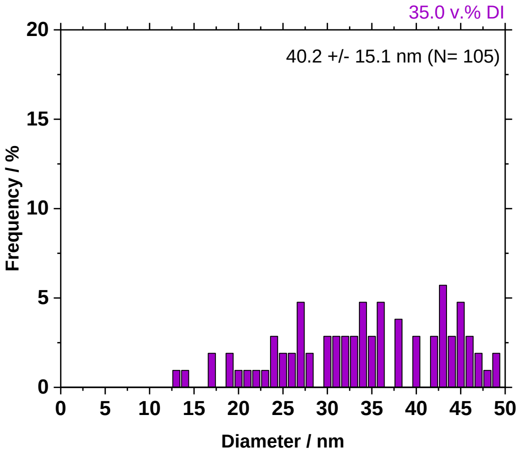
35.0 v.% DI
40.2 +/- 15.1 nm (N= 105)
Frequency / %
Diameter / nm
0
5
10
15
20
0
5
10
15
20
25
30
35
40
45
50

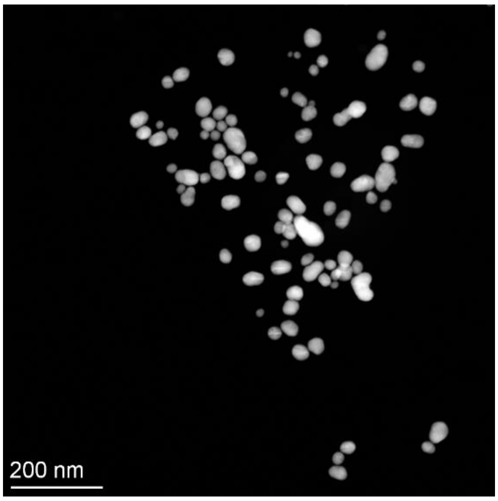
200 nm

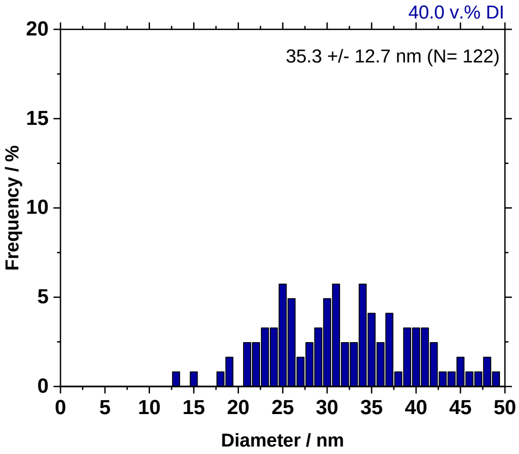
40.0 v.% DI
35.3 +/- 12.7 nm (N= 122)
Frequency / %
Diameter / nm
0
5
10
15
20
0
5
10
15
20
25
30
35
40
45
50

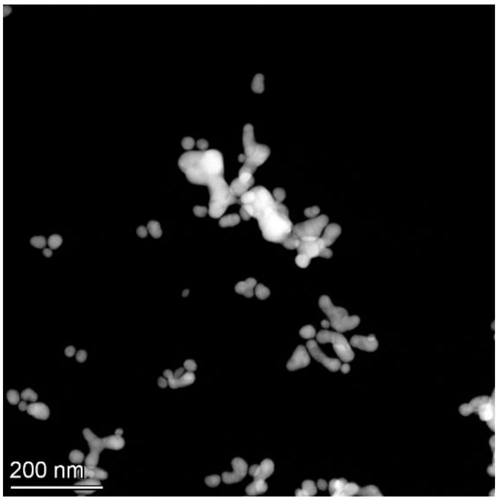
200 nm

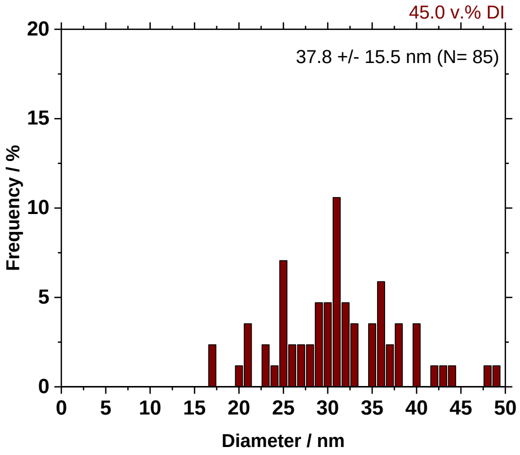
45.0 v.% DI
37.8 +/- 15.5 nm (N= 85)
Frequency / %
Diameter / nm
0
5
10
15
20
0
5
10
15
20
25
30
35
40
45
50

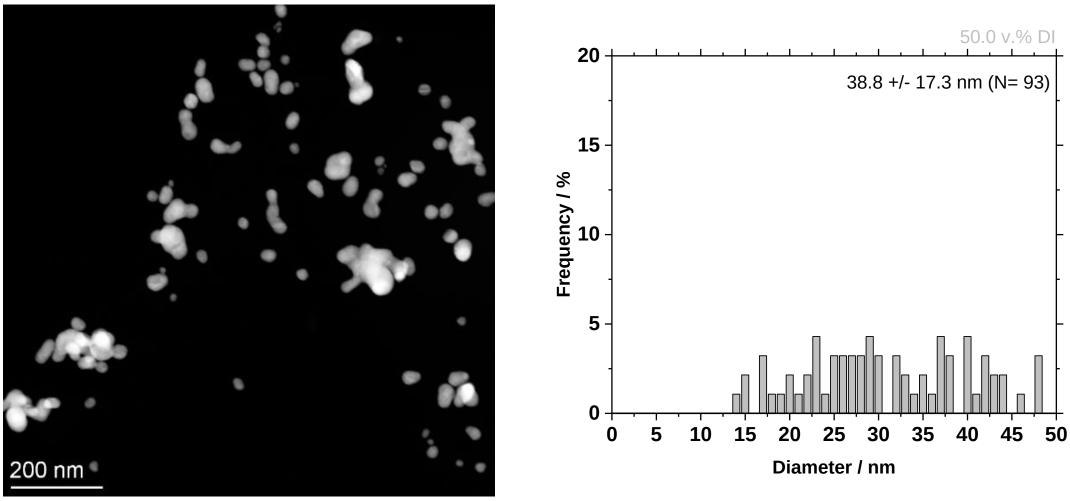

Figure S5. LEFT: Illustrative STEM micrographs of the Au nanomaterials obtained for various DI water content, as indicated. RIGHT: Corresponding size distribution, average size and size distribution, as indicated. Low purity ethanol ($E_{70\%}$) ethanol was used as stock solution of ethanol for all experiments at a final content of 20 v.% for a total of 80 v.% water (DI+mQ). 0.5 mM $HAuCl_4$ and 2 mM NaOH were used in all cases.

Table S2. Overview of the NP typical size retrieved from STEM analysis. The samples for STEM were prepared a day after synthesis. Low purity ethanol ($E_{70\%}$) was used as stock solution of ethanol for all experiments at a final content of 20 v.% for a total of 80 v.% water (DI+mQ). 0.5 mM $HAuCl_4$ and 2 mM NaOH were used in all cases.

DI v.%	**Size** nm	**Deviation** nm	**N**	**General shape**
0.0	10.8	3.4	201	Spherical
2.5	10.1	3.7	174	Spherical
5.0	13.1	5.3	158	Spherical
7.5	11.1	4.1	179	Spherical
10.0	12.5	5.0	150	Spherical
12.5	15.7	5.0	175	Spherical
15.0	14.9	4.7	202	Spherical
17.5	16.5	5.4	150	Spherical
20.0	18.8	7.1	106	Spherical
25.0	18.9	6.2	136	Spherical
30.0	26.2	8.6	118	Some not well defined shapes
35.0	40.2	15.1	105	Less well defined shapes
40.0	35.3	12.7	122	Less well defined shapes
45.0	37.8	15.5	85	Less well defined shapes
50.0	38.8	17.3	93	Less well defined shapes

6- Reproduced results

The datasets discussed in **sections S3-S5** were obtained by an experienced researcher (8 years after PhD). The dataset below was obtained by 3 BSc students with no previous experience with NP synthesis who spent only ca. a week of training (ca. 4 hours a week for 5 weeks) before performing the reported experiments.

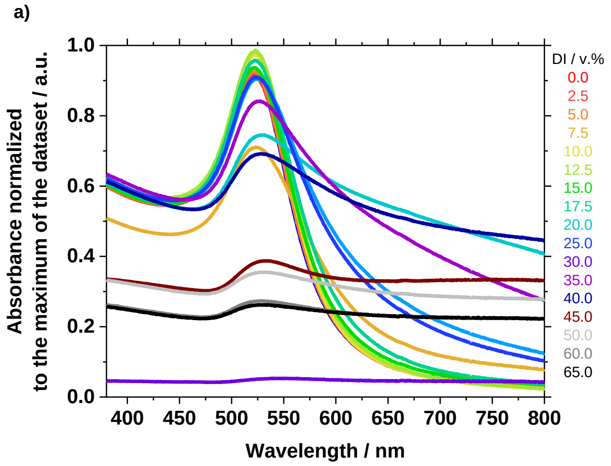

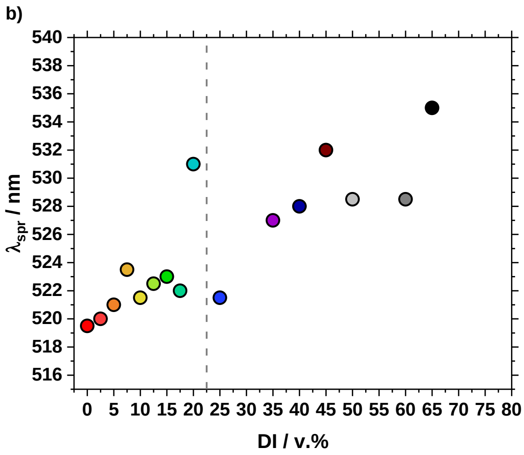

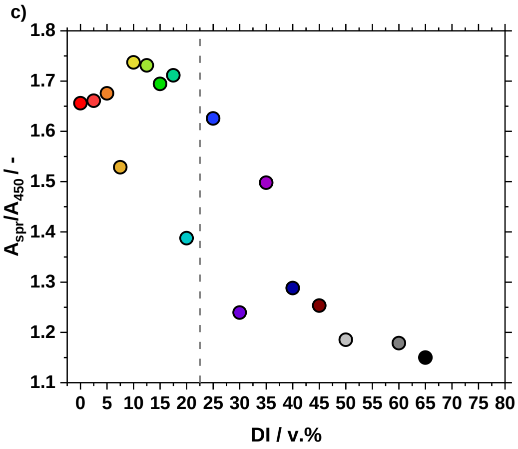

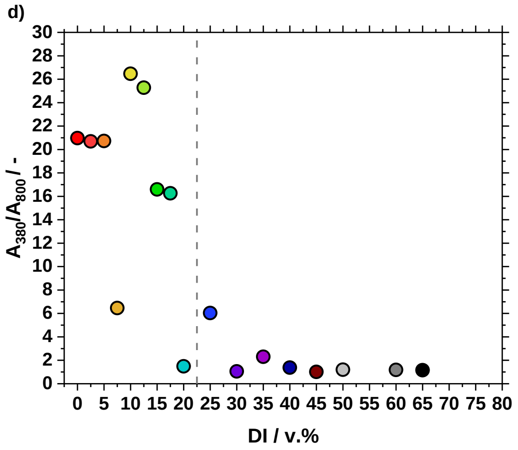

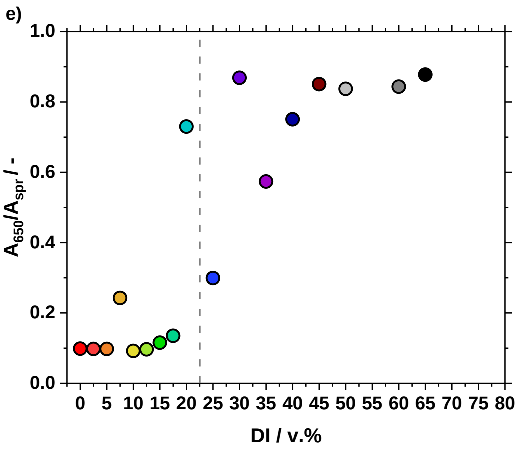

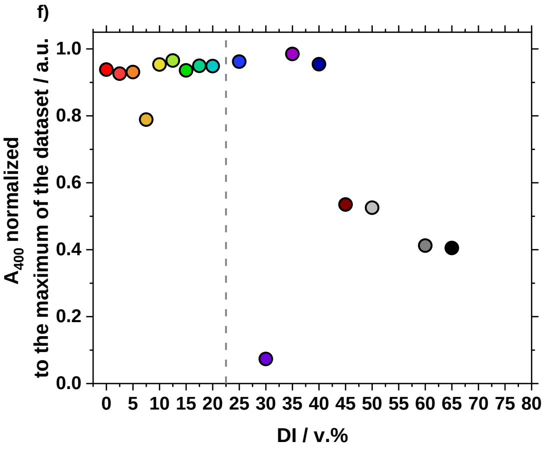

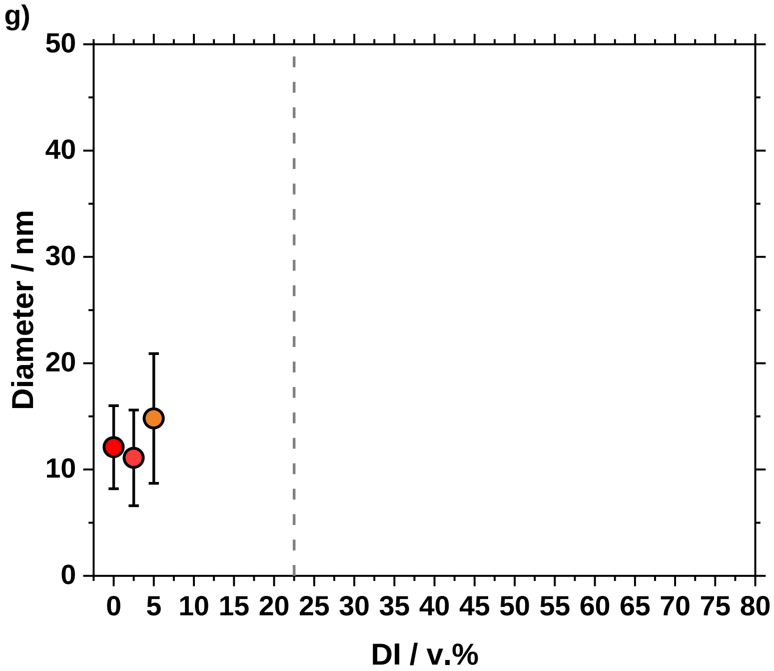

Figure S6. (a) UV-vis spectra of Au NP dispersions obtained using different v.% of DI water, as indicated. (b-f) Various metrics retrieved from UV-vis as a function of DI water content: (b) λ_{spr}, (c) A_{spr}/A_{450}, (d) A_{380}/A_{800}, (e) A_{650}/A_{spr}, and (f) A_{400} (normalized). (g) Diameter retrieved from STEM analysis as a function of DI water content. Only the smallest NPs were considered here. The dotted vertical line indicates the value of 22.5 v.% DI water (to ease the comparison with other plots in this document). Low purity ethanol ($E_{70\%}$) was used as stock solution of ethanol for all experiments at a final content of 20 v.% for a total of 80 v.% water (DI+mQ). 0.5 mM $HAuCl_4$ and 2 mM NaOH were used in all cases.

The samples obtained with 7.5 v.% DI water and 20 v.% DI water appear as outsiders. This is especially clear from the UV-vis spectra in **Figure S6a**, where an overall lower absorbance is measured for 7.5 v.% DI water, which can be attributed to an error in the addition of the $HAuCl_4$ given the relatively small volume to handle (20 µL). The sample prepared at 20 v.% shows a pronounced tail in the UV-vis measurements and a poorly defined spr peak. This outsider is likely coming from experimental errors, among which the possible presence of dust in the cuvette used as reactor, if I was not de-dusted properly can account for lack of reproducibility.

Nevertheless, the results obtained by inexperienced researchers (BSc level) confirm the trend discussed in the main article and show that a relatively fine size control is achieved by using up to ca. 20-25 v.% DI water and low purity stock solutions of ethanol ($E_{70\%}$).

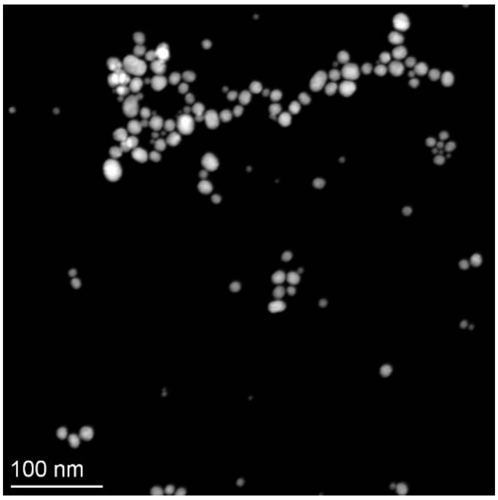
100 nm

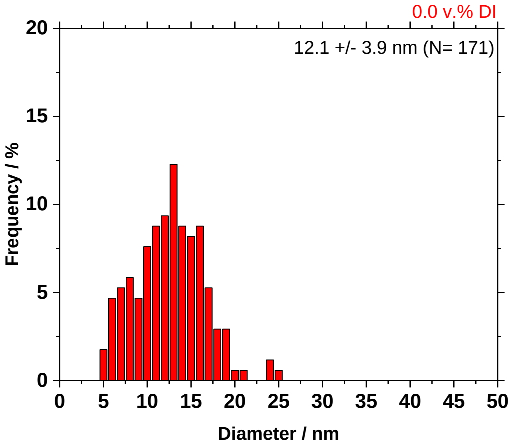
0.0 v.% DI
12.1 +/- 3.9 nm (N= 171)
Frequency / %
Diameter / nm
0
5
10
15
20
25
30
35
40
45
50

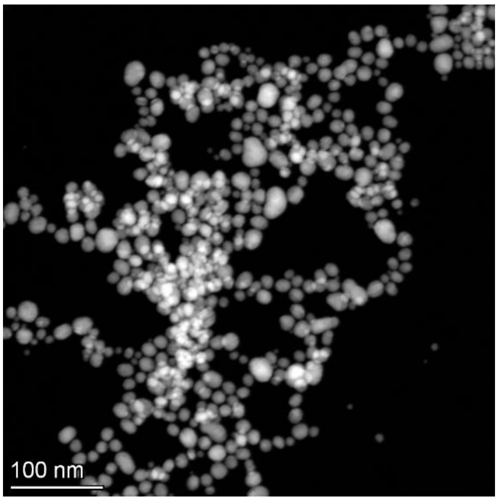
100 nm

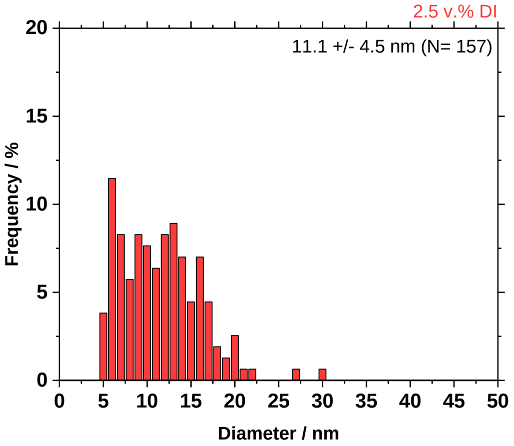
2.5 v.% DI
11.1 +/- 4.5 nm (N= 157)
Frequency / %
Diameter / nm
0
5
10
15
20
25
30
35
40
45
50

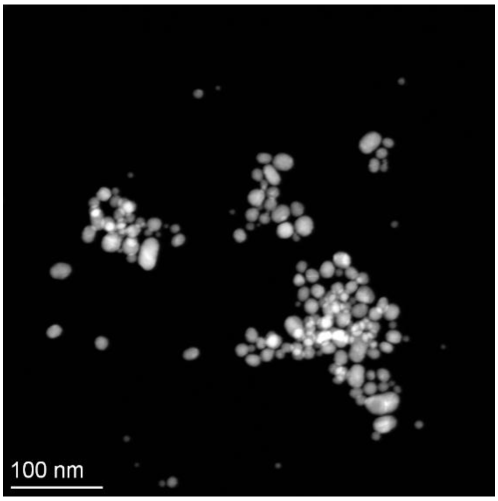
100 nm

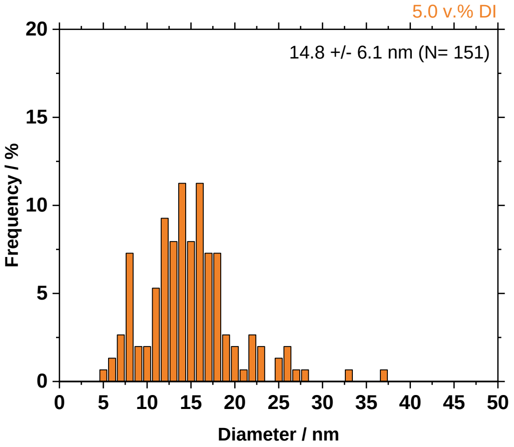
5.0 v.% DI
14.8 +/- 6.1 nm (N= 151)
Frequency / %
Diameter / nm
0
5
10
15
20
25
30
35
40
45
50

Figure S7. LEFT: Illustrative STEM micrographs of the Au nanomaterials obtained for various DI water contents, as indicated. RIGHT: Corresponding size distribution, average size and size distribution, as indicated. Low purity ethanol ($E_{70\%}$) was used as stock solution of ethanol for all experiments at a final content of 20 v.% for a total of 80 v.% water (DI+mQ). 0.5 mM $HAuCl_4$ and 2 mM NaOH were used in all cases. Only the three smallest size samples were characterized by STEM in this case.

Table S3. Overview of the NP typical size retrieved from STEM analysis. The samples for STEM were prepared 2 days after synthesis. Low purity ($E_{70\%}$) ethanol was used as stock solution of ethanol for all experiments at a final content of 20 v.% for a total of 80 v.% water (DI+mQ). 0.5 mM $HAuCl_4$ and 2 mM NaOH were used in all cases.

DI v.%	**Size** nm	**Deviation** nm	**N**	**General shape**
0.0	12.1	3.9	171	Spherical
2.5	11.1	4.5	157	Spherical
5.0	14.8	6.1	151	Spherical

7- Higher purity ethanol

Results in this section were obtained using absolute ethanol ($E_{99.8\%}$) for the synthesis, as a higher grade ethanol source. This is expected to lead to more reproducible and robust results, however at the cost of using a more expensive chemical. The results were obtained by 3 BSc students with no previous experience with NP synthesis that spent ca. a week of training (ca. 4 hours a week for 5 weeks) before performing the reported experiments.

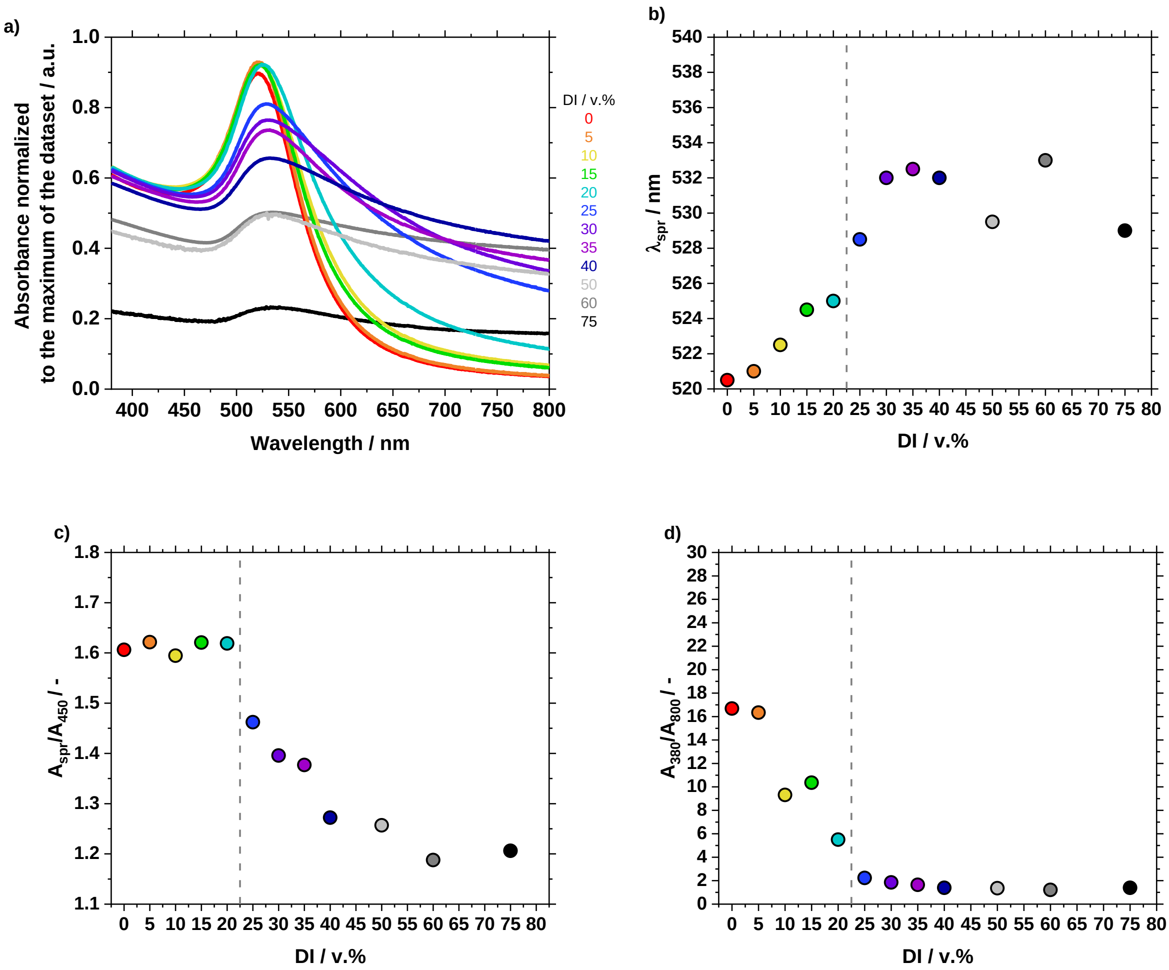

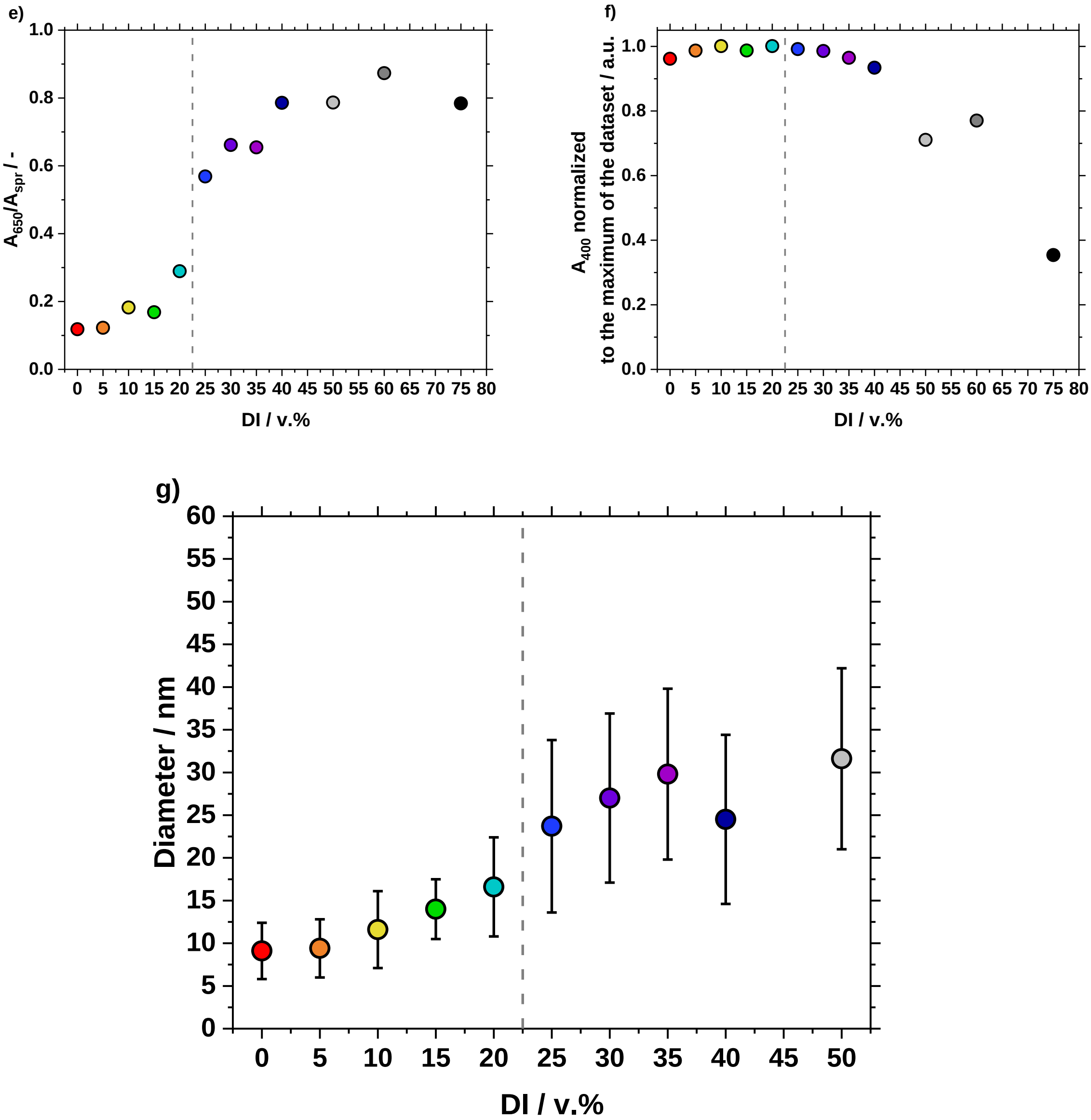

Figure S8. (a) UV-vis spectra of Au NP dispersions obtained using different v.% of DI water, as indicated. (b-f) Various metrics retrieved from UV-vis as a function of DI water content: (b) λ_{spr}, (c) A_{spr}/A_{450}, (d) A_{380}/A_{800}, (e) A_{650}/A_{spr}, and (f) A_{400} (normalized). (g) Diameter retrieved from STEM analysis as a function of DI water content. The dotted vertical line corresponds to the value of 22.5 v.% DI water which indicates the point where the NPs tend to stop being spherical at higher DI contents, as detailed in **Figure S7**. High purity absolute ethanol ($E_{99.8\%}$) was used as stock solution of ethanol for all experiments at a final content of 20 v.% for a total of 80 v.% water (DI+mQ). 0.5 mM $HAuCl_4$ and 2 mM NaOH were used in all cases.

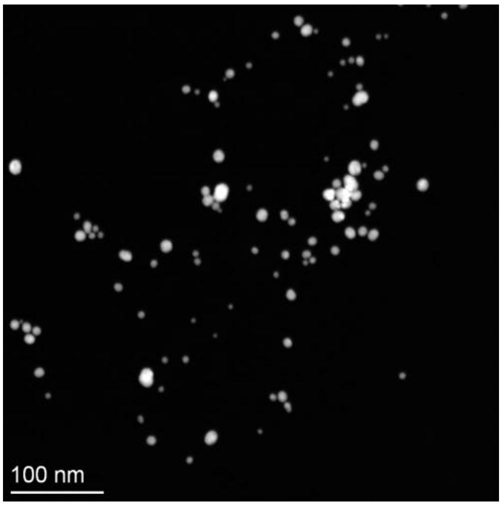
100 nm

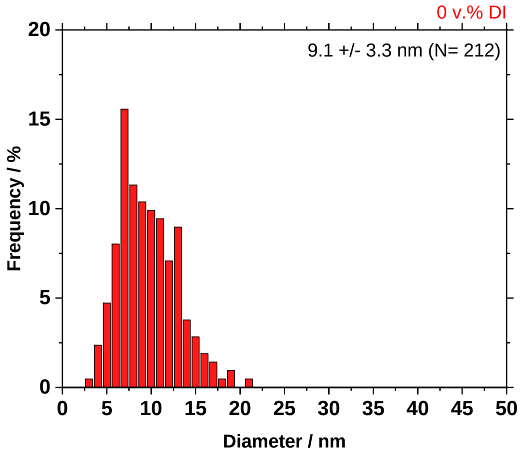
0 v.% DI
9.1 +/- 3.3 nm (N= 212)
Frequency / %
0
5
10
15
20
Diameter / nm
0
5
10
15
20
25
30
35
40
45
50

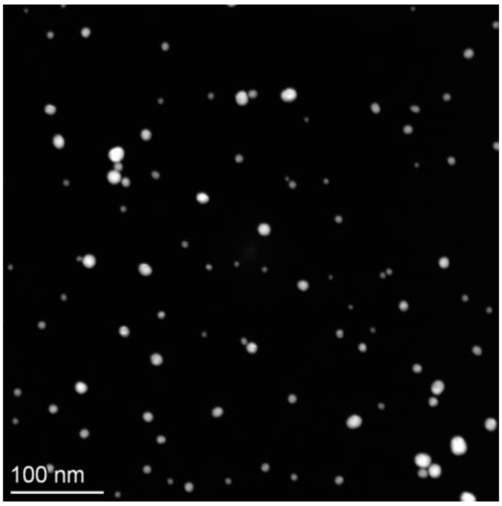
100 nm

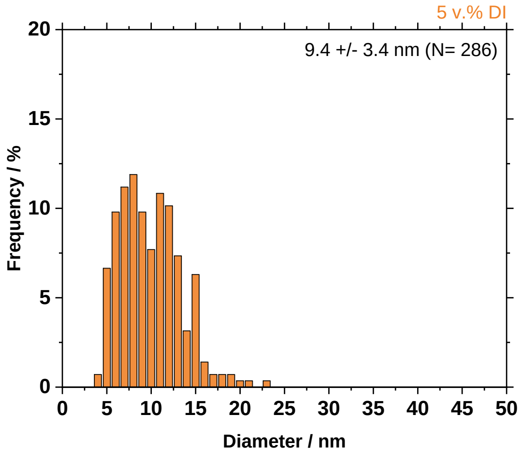
5 v.% DI
9.4 +/- 3.4 nm (N= 286)
Frequency / %
0
5
10
15
20
Diameter / nm
0
5
10
15
20
25
30
35
40
45
50

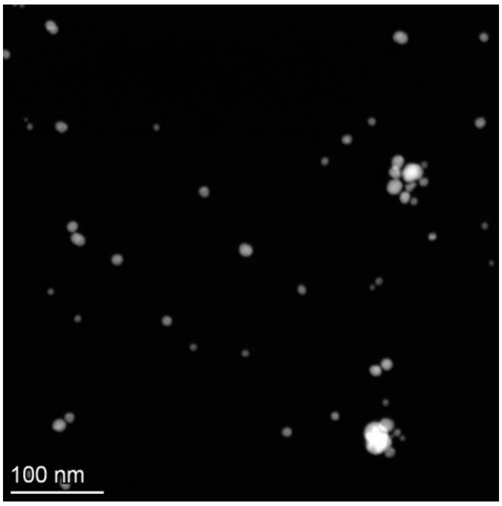
100 nm

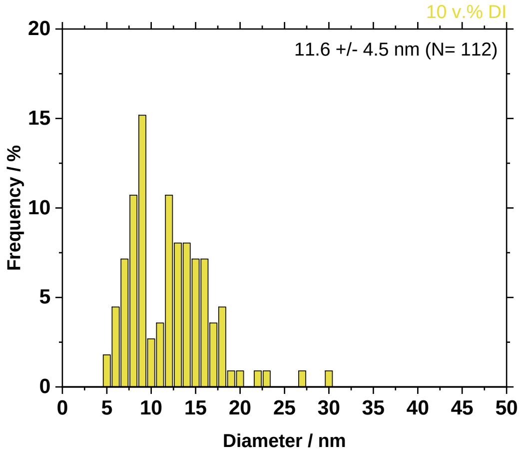
10 v.% DI
11.6 +/- 4.5 nm (N= 112)
Frequency / %
0
5
10
15
20
Diameter / nm
0
5
10
15
20
25
30
35
40
45
50

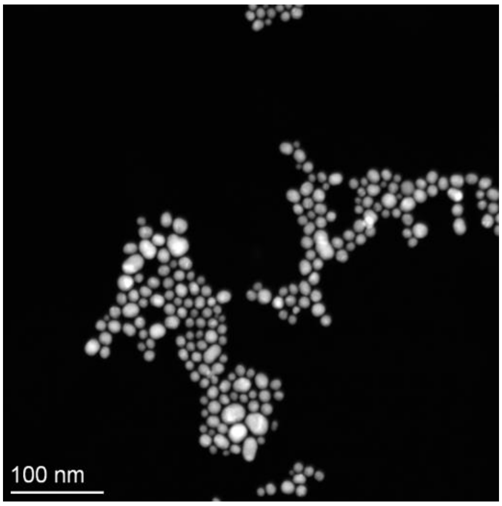
100 nm

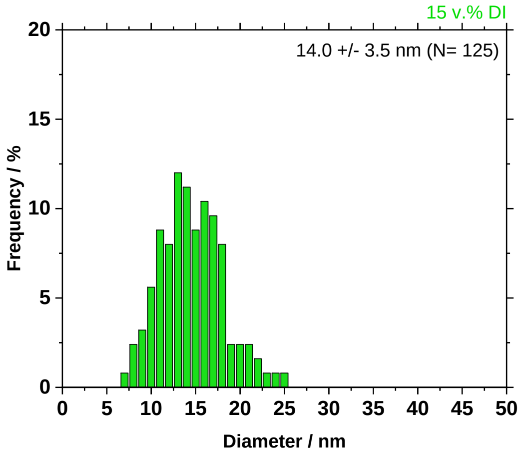
15 v.% DI
14.0 +/- 3.5 nm (N= 125)
Frequency / %
0
5
10
15
20
Diameter / nm
0
5
10
15
20
25
30
35
40
45
50

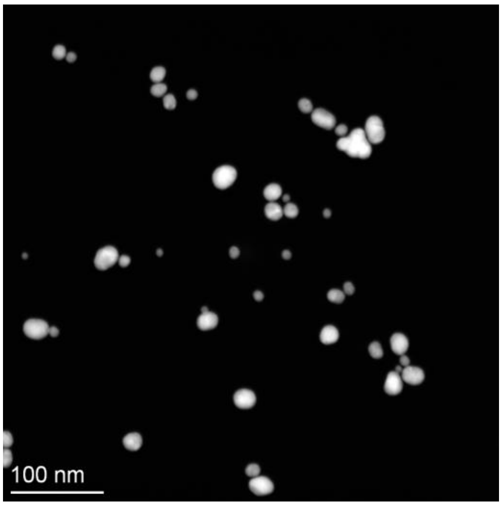
100 nm

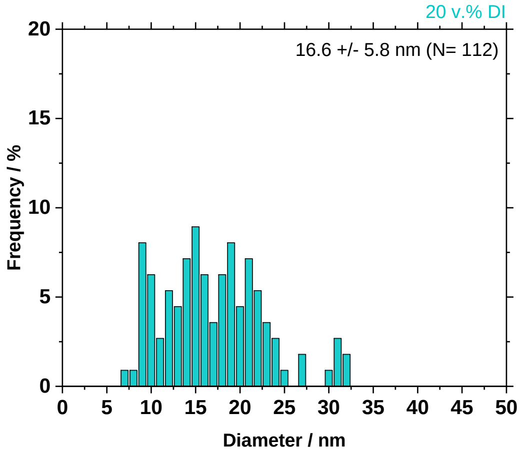
20 v.% DI
16.6 +/- 5.8 nm (N= 112)
Frequency / %
0
5
10
15
20
Diameter / nm
0
5
10
15
20
25
30
35
40
45
50

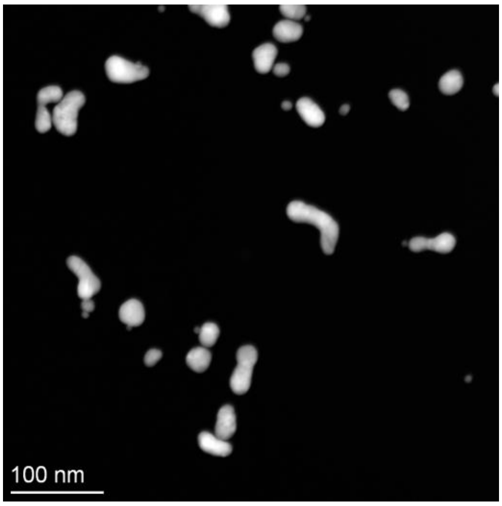
100 nm

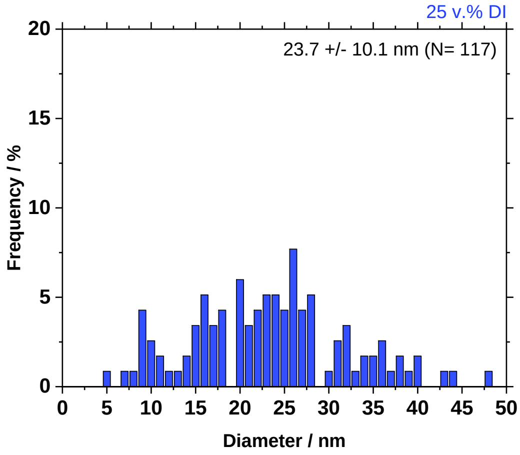
25 v.% DI
23.7 +/- 10.1 nm (N= 117)
Frequency / %
0
5
10
15
20
Diameter / nm
0
5
10
15
20
25
30
35
40
45
50

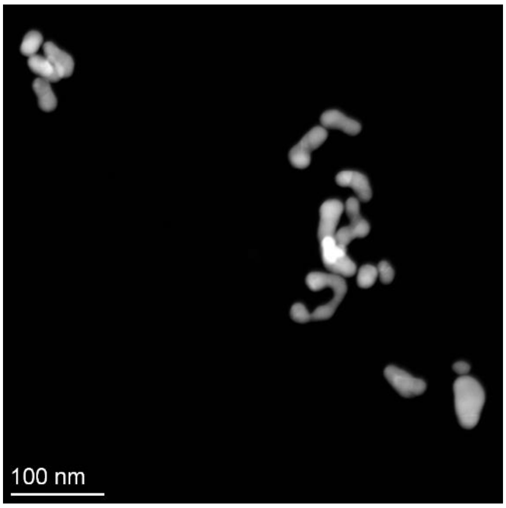
100 nm

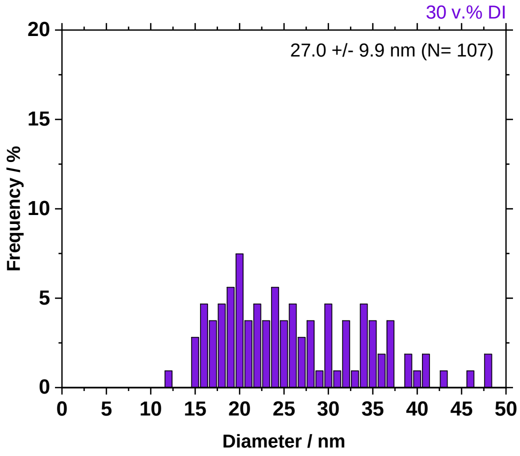
30 v.% DI
27.0 +/- 9.9 nm (N= 107)
Frequency / %
Diameter / nm
0
5
10
15
20
0
5
10
15
20
25
30
35
40
45
50

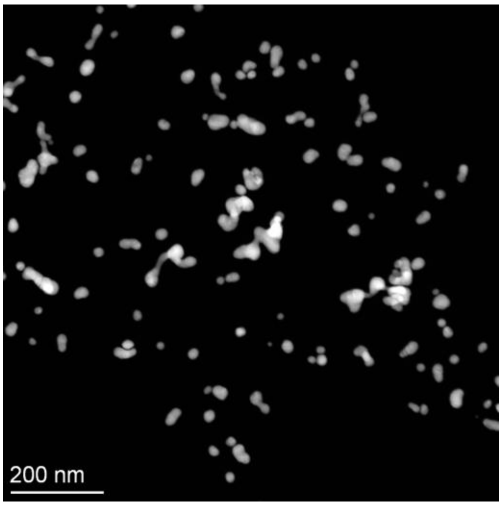
200 nm

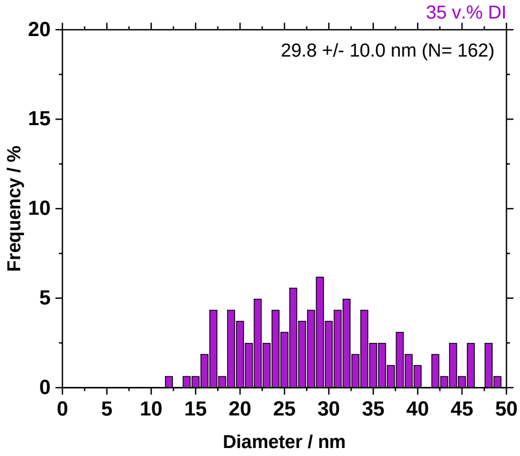
35 v.% DI
29.8 +/- 10.0 nm (N= 162)
Frequency / %
Diameter / nm
0
5
10
15
20
0
5
10
15
20
25
30
35
40
45
50

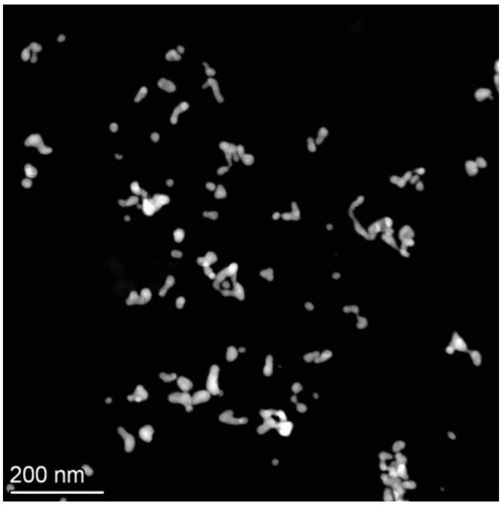
200 nm

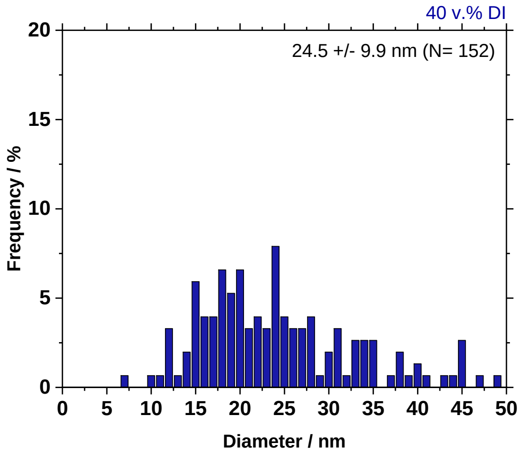
40 v.% DI
24.5 +/- 9.9 nm (N= 152)
Frequency / %
Diameter / nm
0
5
10
15
20
0
5
10
15
20
25
30
35
40
45
50

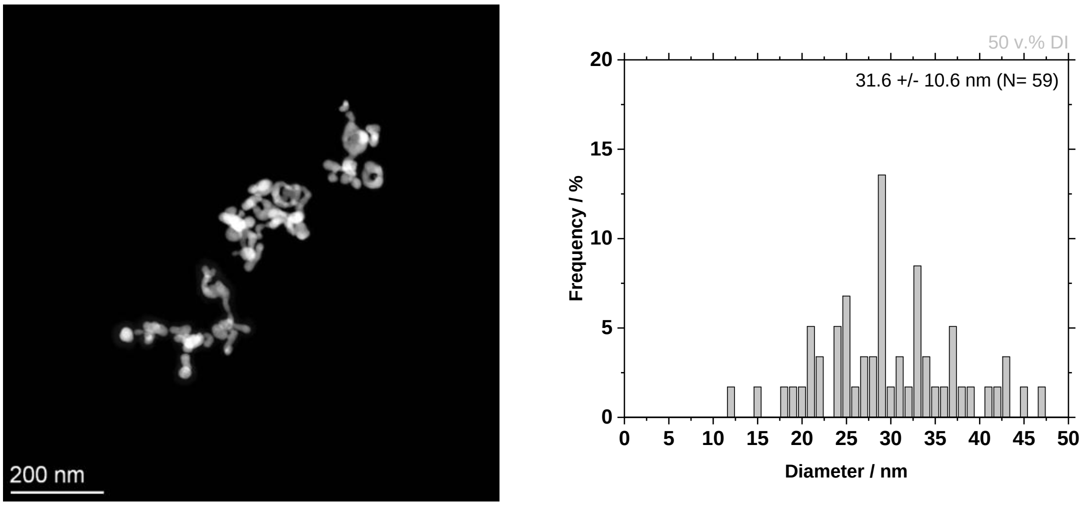

Figure S9. LEFT: Illustrative STEM micrographs of the Au nanomaterials obtained for various DI water content, as indicated. RIGHT: Corresponding size distribution, average size and size distribution, as indicated. High purity absolute ethanol ($E_{99.8\%}$) was used as stock solution of ethanol for all experiments at a final content of 20 v.% for a total of 80 v.% water (DI+mQ). 0.5 mM $HAuCl_4$ and 2 mM NaOH were used in all cases.

Table S4. Overview of the NP typical size retrieved from STEM analysis. The samples for STEM were prepared a week after synthesis. High purity absolute ethanol ($E_{99.8\%}$) was used as stock solution of ethanol for all experiments at a final content of 20 v.% for a total of 80 v.% water (DI+mQ). 0.5 mM $HAuCl_4$ and 2 mM NaOH were used in all cases.

DI v.%	**Size** nm	**Deviation** nm	**N**	**General shape**
0	9.1	3.3	212	Spherical
5	9.4	3.4	286	Spherical
10	11.6	4.5	112	Spherical
15	14.0	3.5	125	Spherical
20	16.6	5.8	112	Spherical
25	23.7	10.1	117	Some not well defined shapes
30	27.0	9.9	107	Less well defined shapes
35	29.8	10	162	Less well defined shapes
40	24.5	9.9	152	Less well defined shapes
50	31.6	10.6	59	Less well defined shapes

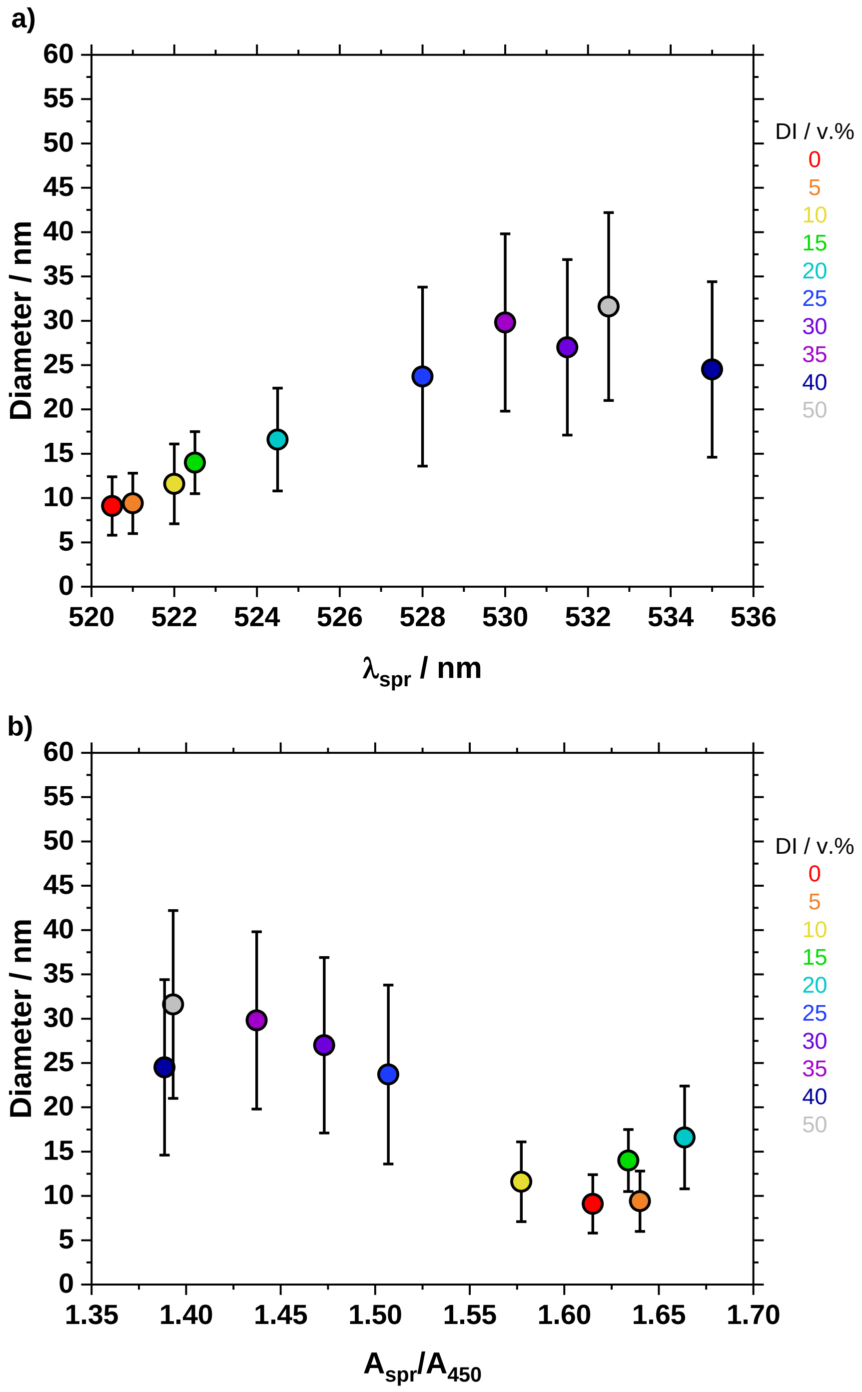

Figure S10. Examples of relationships between size and UV-vis metrics: (a) λ_{spr} and (b) A_{spr}/A_{450}. The corresponding content of DI water for each data point is as indicated. High purity absolute ethanol ($E_{99.8\%}$) was used as stock solution of ethanol for all experiments at a final content of 20 v.% for a total of 80 v.% water (DI+mQ). 0.5 mM $HAuCl_4$ and 2 mM NaOH were used in all cases.

For the size range considered and the solvent mixture used here, there is a better correlation between higher λ_{spr} values and larger NPs, compared to the trend that higher A_{spr}/A_{450} ratios correlate with larger size NPs, which can be attributed to the fact that in the present case, for A_{spr}/A_{450} ratios lower than ca. 1.55, the corresponding sample do not display spherical NPs as detailed in **Figure S9**.

8-Polyol-based syntheses

Alcohol-mediated surfactant-free (SF) RT syntheses of Au NPs can also be performed using polyols such as glycerol[26] or ethylene glycol.[27] However, both are rather viscous solvents, which can complicate the work-up of the as-prepared Au NPs (e.g. need of waste-generating steps such as acid cleaning).[28,29] We also showed that the robustness of the synthesis, i.e. the experimental window for which the synthesis leads to small size Au NPs upon varying the amount of base and/or alcohol content, is larger for glycerol than for ethylene glycol, itself larger than for ethanol. We here assessed the possibility to obtain Au NPs using DI water in mQ water using glycerol and ethylene glycol. Results are reported in **Figure S10**.

Considering the UV-vis spectra and various metrics reported as a function of the amount of DI water, it can be concluded that the use of polyols leads to syntheses that are less sensitive to the amount of DI water. This is attributed to the properties of polyols leading to overall faster synthesis and to more viscous media likely to stabilize the NPs.[5] Nevertheless, the viscous media prevent a readily use of the as-prepared Au NPs.[29]

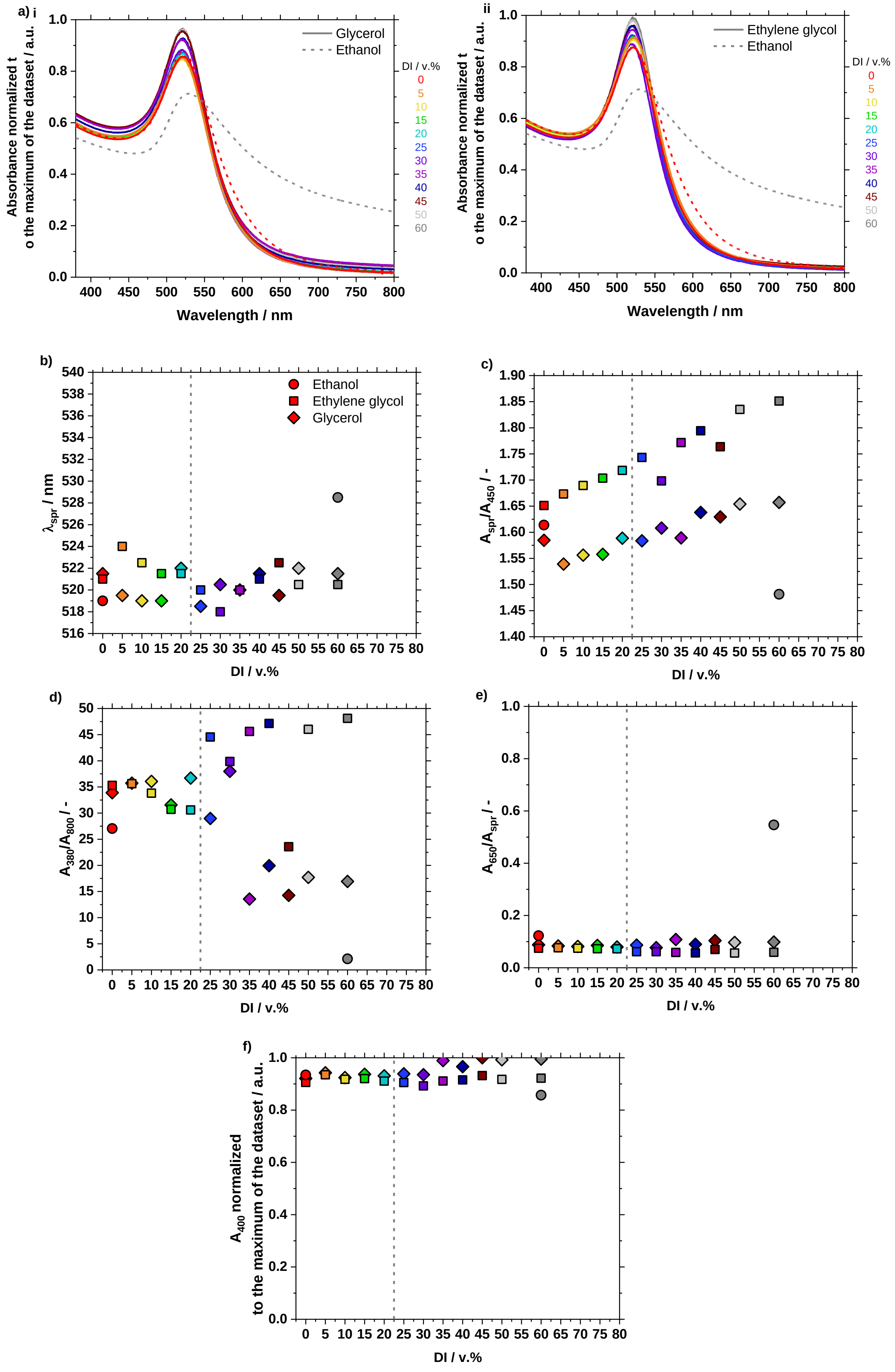
a) i
Absorbance normalized t
o the maximum of the dataset / a.u.
Wavelength / nm
Glycerol
Ethanol
DI / v.%
0
5
10
15
20
25
30
35
40
45
50
60
ii
Ethylene glycol
Ethanol
b)
λ_{spr} / nm
DI / v.%
Ethanol
Ethylene glycol
Glycerol
c)
A_{spr}/A_{450} / -
d)
A_{380}/A_{800} / -
e)
A_{650}/A_{spr} / -
f)
A_{400} normalized
to the maximum of the dataset / a.u.

Figure S11. (a) UV-vis spectra of Au NP dispersions obtained using different v.% of DI water, as indicated, using (i, left) glycerol or (ii, right) ethylene glycol as source of reducing agents. For comparison experiments obtained with 0 v.% and 60 v.% DI water and using ethanol (dashed lines) are reported in both graphs. (b-f) Various metrics retrieved from UV-vis as a function of DI water content when glycerol (◇), ethylene glycol (□) or ethanol (○) for comparison, are used: (b) λ_{spr}, (c) A_{spr}/A_{450}, (d) A_{380}/A_{800}, (e) A_{650}/A_{spr}, and (f) A_{400} (normalized). The dotted vertical line corresponds to the value of 22.5 v.% DI water (to ease the comparison with other plots in this document). High purity absolute ethanol ($E_{99.8\%}$) was used as stock solution of ethanol. The final content of alcohol was 20 v.% in all cases and 80 v.% water (DI+mQ). 0.5 mM $HAuCl_4$ and a NaOH/Au molar ratio of 4.0 were used in all cases.

9-Stability

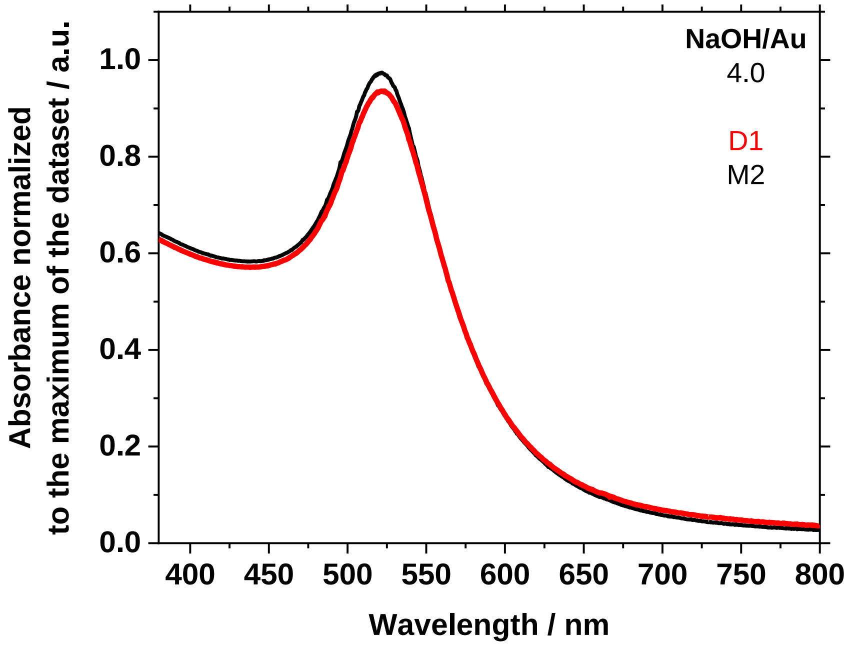

Figure S12. UV-vis spectra of Au NP colloidal dispersion obtained with 80 v.% mQ water, 0.5 mM $HAuCl_4$ and a NaOH/Au molar ratio of 4.0. The samples were left on a bench at RT and ambient light. The UV-vis spectra recorded the day after the synthesis (D1) and 2 months (M2) after the synthesis (the sample was not shaken for homogenization) are reported. High purity absolute ethanol ($E_{99.8\%}$) was used as stock solution of ethanol at a final content of 20 v.%.

The results illustrate the stability of the Au NPs even when stored at ambient light. The slightly higher value at for A_{400} is attributed to solvent evaporation that might concentrate the Au NPs.

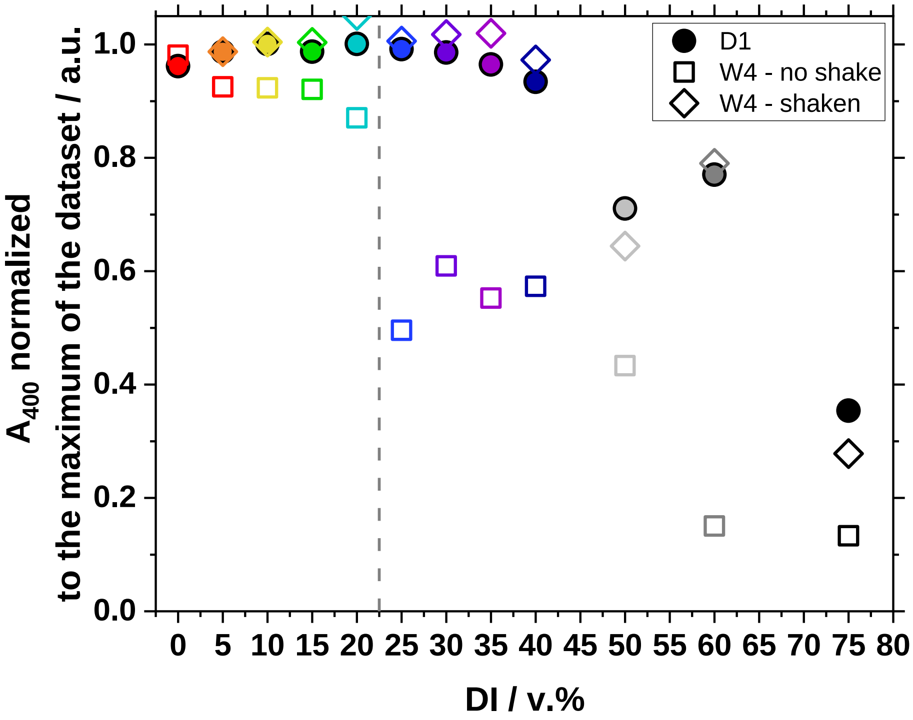

Figure S13. Illustration of the stability of the Au NPs dispersions comparing as-prepared colloidal dispersions (D1, ●), dispersions measured after 4 weeks (W4) as they are (no shake, □) and after a gentle shake to re-disperse the NPs (shaken, ◇). The value of A_{400} of the as-prepared colloidal Au NP dispersions is taken as reference. High purity absolute ethanol ($E_{99.8\%}$) was used as stock solution of ethanol for all experiments at a final content of 20 v.% for a total of 80 v.% water (DI+mQ). 0.5 mM $HAuCl_4$ and 2 mM NaOH were used in all cases.

The results that the colloidal dispersions with higher DI water contents are less stable over time (in agreement with the stability factors detailed in **Figure S8**) but can easily be re-dispersed by shaking the sample.

It is worth stressing that SF Au NP samples prepared with only mQ are stable for months and even years.[1,4,30]

10- Conductivity

a)

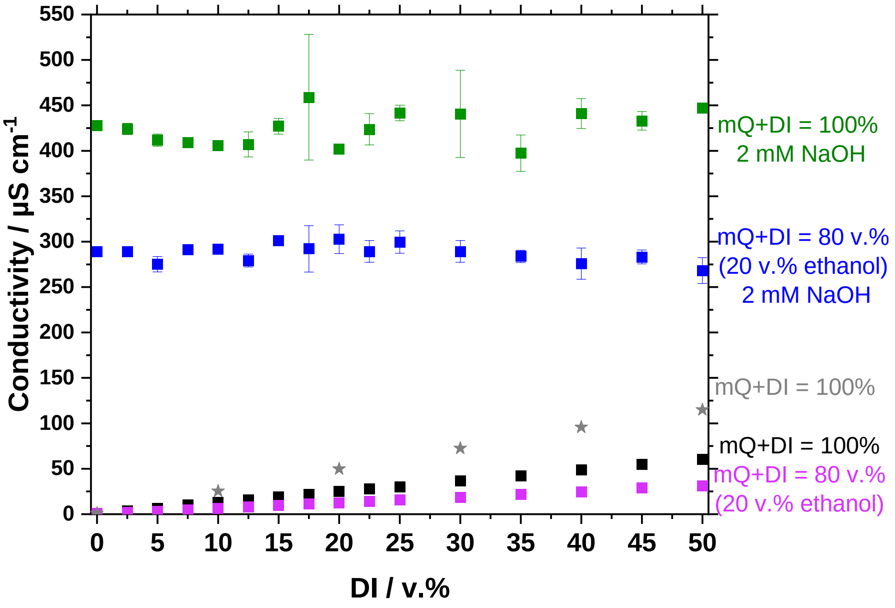

b)

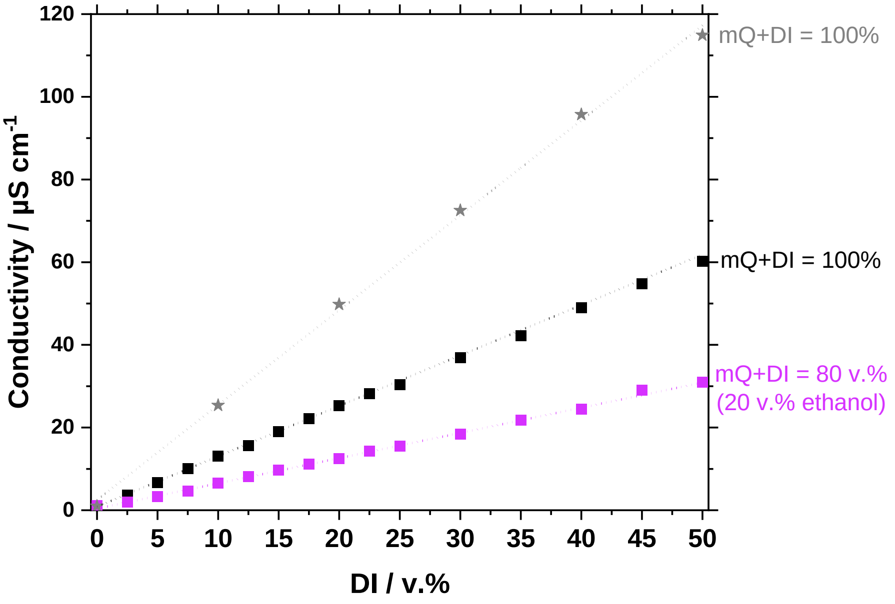

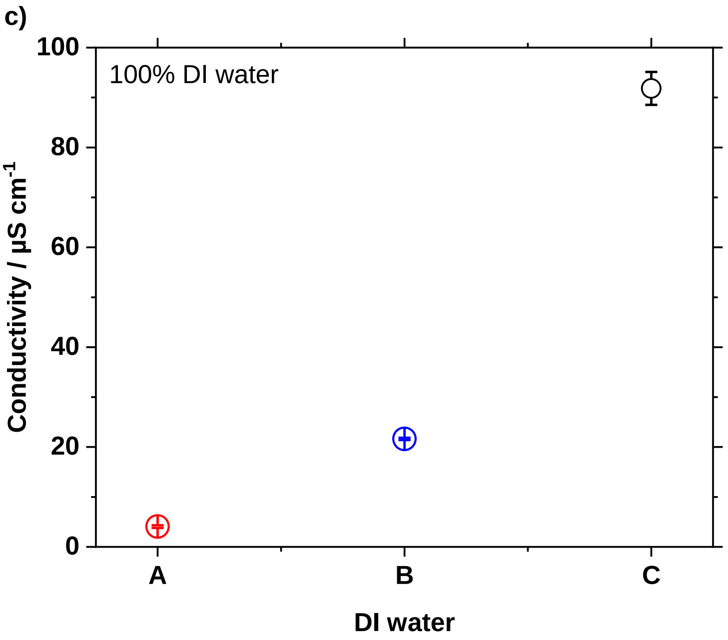

Figure S14. (a, b) Conductivity as a function of the amount of DI water used (were the amount of DI water is here expressed relative to the water fraction of the mixture). (a) For various samples consisting of mQ+DI (100%, no alcohol) with and without 2 mM NaOH, and consisting of mQ+DI for a total of 80 v.% together with 20 v.% ethanol with and without 2 mM NaOH, as indicated. (b) Same data as (a) focusing on the case without NaOH. (c) Conductivity of DI water from different sources (A is from a first building, B and C from a second building, B is on a given day and C on another day). The sample corresponding to B was used for this study.

The conductivity measurements show, as expected, that in presence of NaOH most of the conductivity comes from NaOH and there is little dependence on the amount of DI water. Without NaOH, the conductivity increases linearly with the amount of DI water. Interestingly, the slope observed on different days (black and grey datasets) is different. This is attributed to variations in the conductivity of DI water in our supply as illustrated in **Figure S14c**. We also observed that the conductivity of DI water is different for different buildings at Aarhus University in the range 4 to 91 µS cm^{-1}. This result stresses the importance of controlled water and stresses the preference for mQ water in the literature. Those results also stress that the strategy to add DI water to control NP size will likely require different amounts of DI water to be added depending on the conductivity of the stock of DI water. Note that for the experiments reported here, the same stock of DI water was used (21.5 µS cm^{-1}).

11- 4-NP reduction

Abbreviations. In the following, **Figure S15-S17**, the TOF_t corresponds to the TOF estimated after a given reaction time as indicated in **Table S5**. $TOF_{t\text{-}A400}$ corresponds to the TOF_t normalized by the A_{400} value retrieved from UV-vis of the as-prepared colloidal Au NPs (absorbance at 400 nm). $TOF_{\%}$ corresponds to the TOF estimated considering the maximum conversion reached for the total duration of the experiments as indicated in **Table S5**. $TOF_{\%\text{-}A400}$ corresponds to the $TOF_{\%}$ normalized by the A_{400} value.

Comment on literature. It can be generally challenging to compare the results reported from the literature since various setups, protocols (e.g. concentrations) and metrics can be used and/or reported.[22,31-33] We here focus on the relative performance of the samples. To propose a comparison Au NPs were obtained using $NaBH_4$ without other additives.[6] Those Au NPs were chosen because they were reported to be very active for the 4-NP reduction. To allow a fair comparison NPs in the same size range ca. 10 nm were prepared as detailed in the experimental section.

Comment on experimental setup. In order to comply with the principle of sustainability in the laboratory,[7] we aimed to minimize the volume of 4-NP to use and the kinetics study were performed in UV-vis cuvettes directly placed in a Go Direct® UV-vis spectrophotometer (see **section S1**). The resolution of the equipment is not the highest and we observed that over time during the same day, TOF values tend to increase, which we attributed to the spectrophotometer heating up. The values reported in the manuscript in **Figure 3** and **Figure S17** are reported for samples measured first in the day. The values reported in **Figure S16** are obtained from at least 3 repeats where the order in which the activity of the Au NPs was assessed was permuted to alleviate for this possible experimental error. **Figure S18** confirms the trend observed in **Figure S16**. **Figure S18c** show the typical evolution of $-\ln(A_t/A_0)$, where A_t is the absorbance at 400 nm measured over time, as defined in the experimental section. The rather noisier data for the sample with a size around 12 nm is due to the formation of bubbles in the small volume of 2 mL used for the experiment.

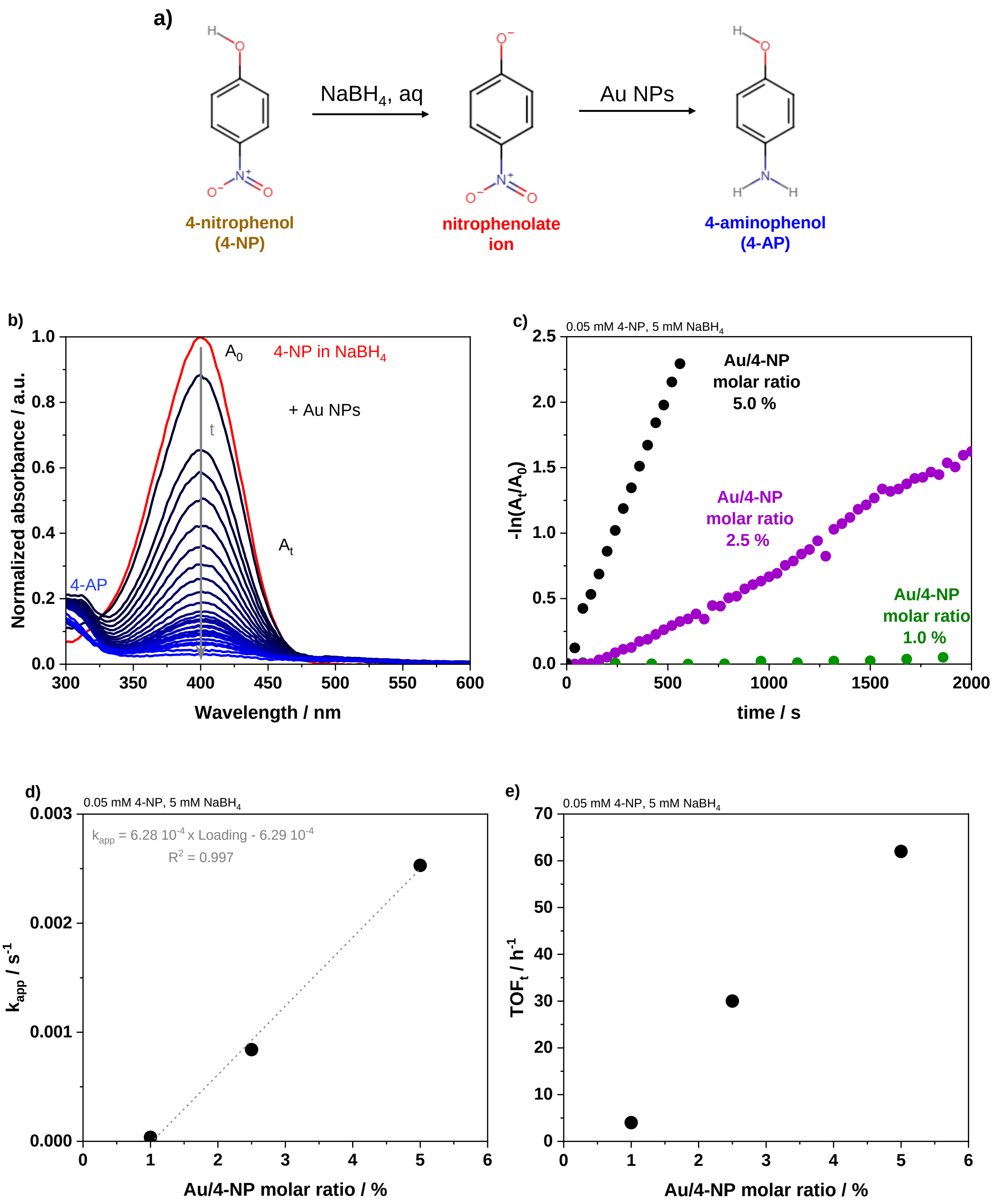

Figure S15. (a) Schematic illustration of 4-NP reduction by Au NPs in presence of $NaBH_4$. The molecular formulas were obtained with the RSCB Protein Data Bank (RSCB PDB), Chemical Sketch Tool, Marvin JS chemical editor tool by Chemaxon. Available at: https://www.rcsb.org/chemical-sketch. (b) Illustrative UV-vis data illustrating the decrease of the absorbance at 400 nm over time in presence of Au NPs. (c) Illustration of the related plot of $-\ln(A_t/A_0)$ as a function of time to retrieve kinetics parameters and TOF as detailed in the experimental section in section S1, here with different Au/4-NP molar ratios, as indicated. (d-e) Effect of the Au loading on 4-NP reduction for (d) k_{app} and (e) TOF_t evaluated at 960s, see **Table S5**. For these experiments, NPs obtained using 0.0 v.% DI water were used.

The results presented are in line with previous reports, e.g. regarding the linear relationship between k_{app} and the catalyst loading (Au/4-NP molar ratio).[22] For the following screening and the experimental conditions used here, we preferred the use of a Au/4-NP molar ratio of 5% in order to minimize the duration of the experiments. Note that the use of a Au/4-NP molar ratio higher than 5% leads to more complex experiments due to the formation of bubbles, detrimental to the acquisition of UV-vis data in the rather small volume of 2 mL used here.

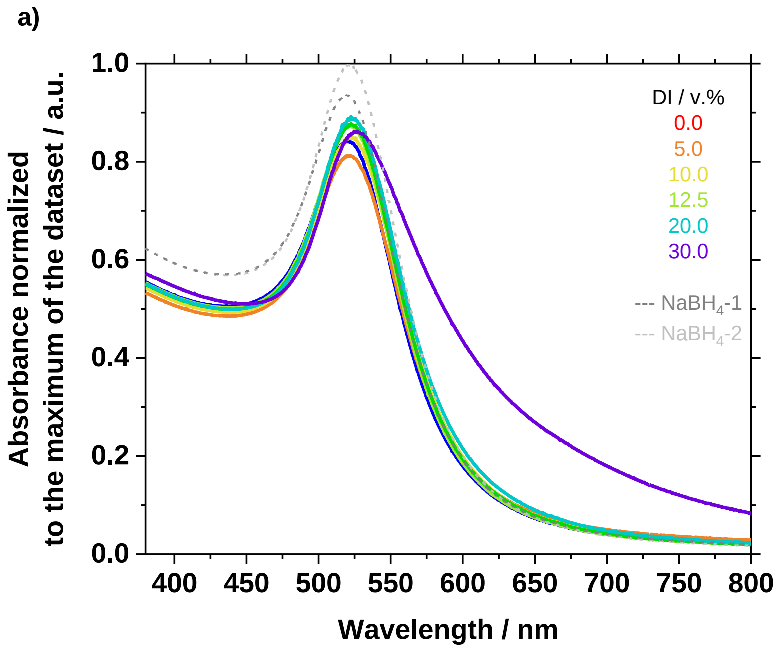
a)
Absorbance normalized to the maximum of the dataset / a.u.
1.0
0.8
0.6
0.4
0.2
0.0
400
450
500
550
600
650
700
750
800
Wavelength / nm
DI / v.%
0.0
5.0
10.0
12.5
20.0
30.0
--- NaBH$_4$-1
--- NaBH$_4$-2

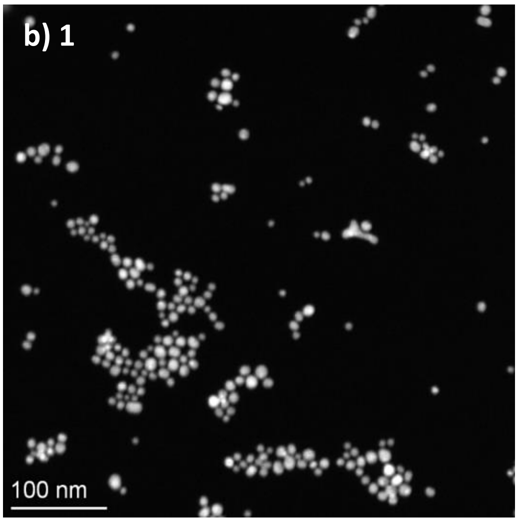
b) 1
100 nm

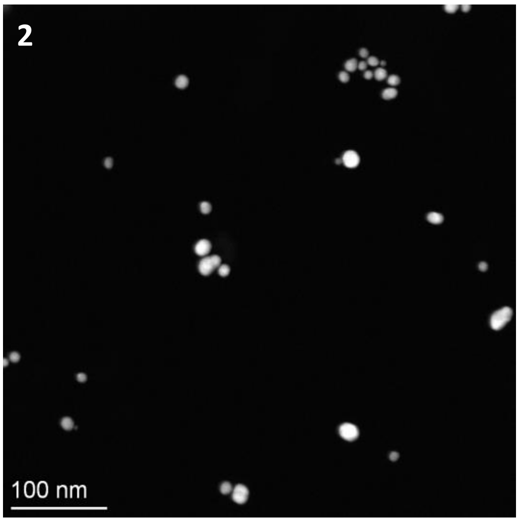
2
100 nm

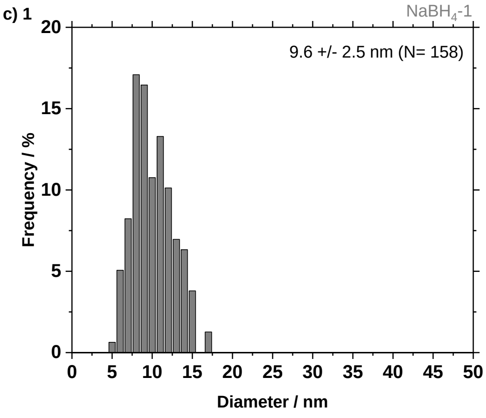
c) 1
NaBH$_4$-1
9.6 +/- 2.5 nm (N= 158)
Frequency / %
20
15
10
5
0
0
5
10
15
20
25
30
35
40
45
50
Diameter / nm

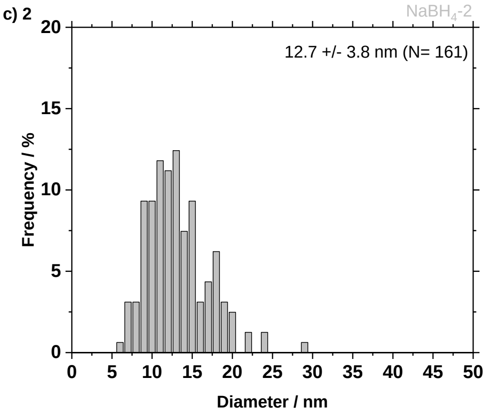
c) 2
NaBH$_4$-2
12.7 +/- 3.8 nm (N= 161)
Frequency / %
20
15
10
5
0
0
5
10
15
20
25
30
35
40
45
50
Diameter / nm

d)

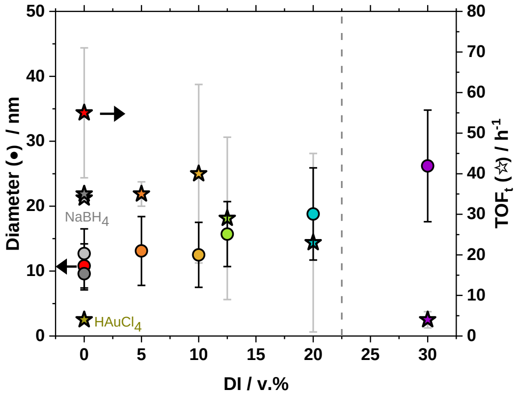
Diameter (●) / nm
0
10
20
30
40
50
TOF_t (☆) / h^-1
0
10
20
30
40
50
60
70
80
NaBH4
HAuCl4
DI / v.%
0
5
10
15
20
25
30

e)

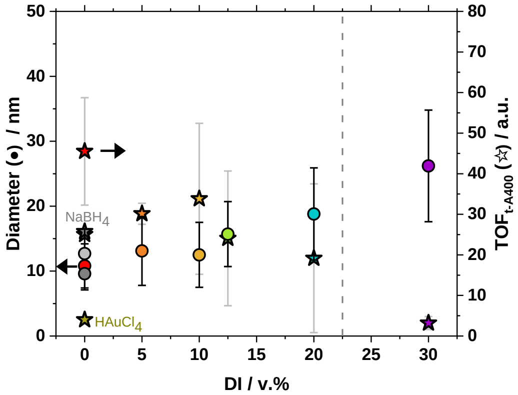
Diameter (●) / nm
0
10
20
30
40
50
TOF_t-A400 (☆) / a.u.
0
10
20
30
40
50
60
70
80
NaBH4
HAuCl4
DI / v.%
0
5
10
15
20
25
30

f)

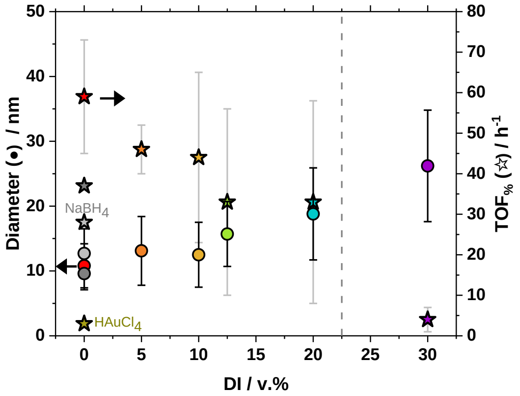
Diameter (●) / nm
0
10
20
30
40
50
TOF_% (☆) / h^-1
0
10
20
30
40
50
60
70
80
NaBH4
HAuCl4
DI / v.%
0
5
10
15
20
25
30

g)

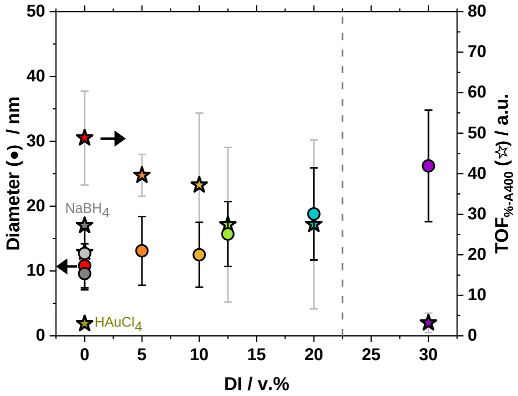
Diameter (●) / nm
0
10
20
30
40
50
TOF_%-A400 (☆) / a.u.
0
10
20
30
40
50
60
70
80
NaBH4
HAuCl4
DI / v.%
0
5
10
15
20
25
30

h)

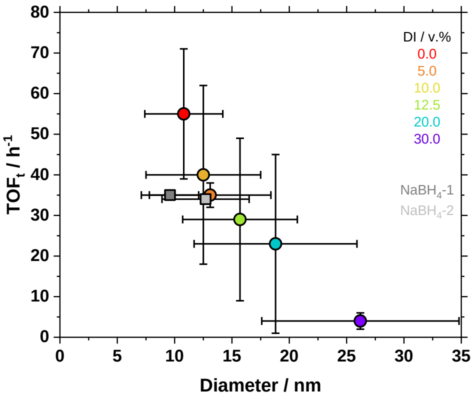
TOF_t / h^-1
0
10
20
30
40
50
60
70
80
DI / v.%
0.0
5.0
10.0
12.5
20.0
30.0
NaBH4-1
NaBH4-2
Diameter / nm
0
5
10
15
20
25
30
35

i)

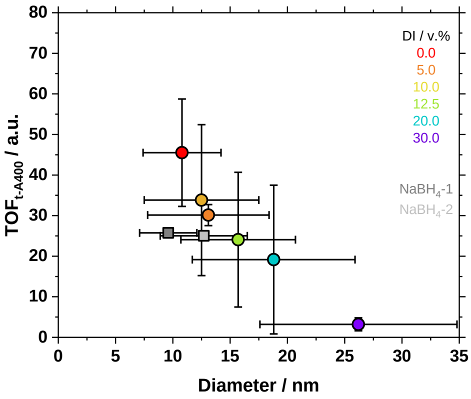
TOF_t-A400 / a.u.
0
10
20
30
40
50
60
70
80
DI / v.%
0.0
5.0
10.0
12.5
20.0
30.0
NaBH4-1
NaBH4-2
Diameter / nm
0
5
10
15
20
25
30
35

j)

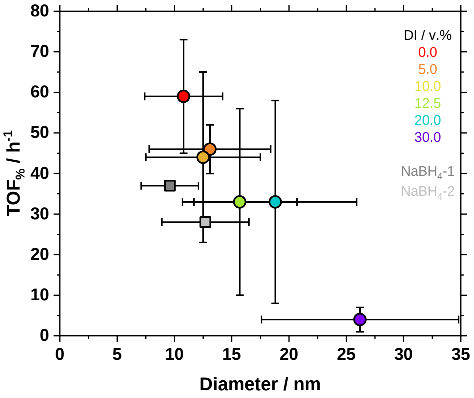
TOF_% / h^-1
0
10
20
30
40
50
60
70
80
DI / v.%
0.0
5.0
10.0
12.5
20.0
30.0
NaBH4-1
NaBH4-2
Diameter / nm
0
5
10
15
20
25
30
35

k)

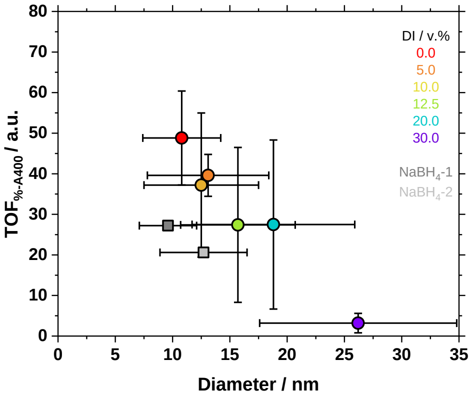
TOF_%-A400 / a.u.
0
10
20
30
40
50
60
70
80
DI / v.%
0.0
5.0
10.0
12.5
20.0
30.0
NaBH4-1
NaBH4-2
Diameter / nm
0
5
10
15
20
25
30
35

Figure S16. (a) Illustrative UV-vis spectra of the Au NPs considered for the 4-NP reduction, obtained with different amounts of DI water, as indicated. Low purity ethanol ($E_{70\%}$) was used as stock solution of ethanol for all experiments at a final content of 20 v.% for a total of 80 v.% water (DI+mQ). 0.5 mM $HAuCl_4$ and 2 mM NaOH were used in all cases. (b) STEM micrograph and (c) related size distribution for Au NPs prepared using $NaBH_4$, samples 1 and 2, $NaBH_4$-1 and $NaBH_4$-2 respectively. (d) TOF_t, (e) $TOF_{t\text{-}A400}$, (f) $TOF_{\%}$, (g) $TOF_{\%\text{-}A400}$ as a function of DI water content. For comparison, the results obtained with Au NPs prepared by $NaBH_4$ and using an equivalent concentration of Au in the form of $HAuCl_4$ are reported (☆) for 0 v.% DI. (h) TOF_t, (i) $TOF_{t\text{-}A400}$, (j) $TOF_{\%}$, (k) $TOF_{\%\text{-}A400}$ as a function of the Au NP size. In all cases the molar ratio Au/4-NP was 5%.

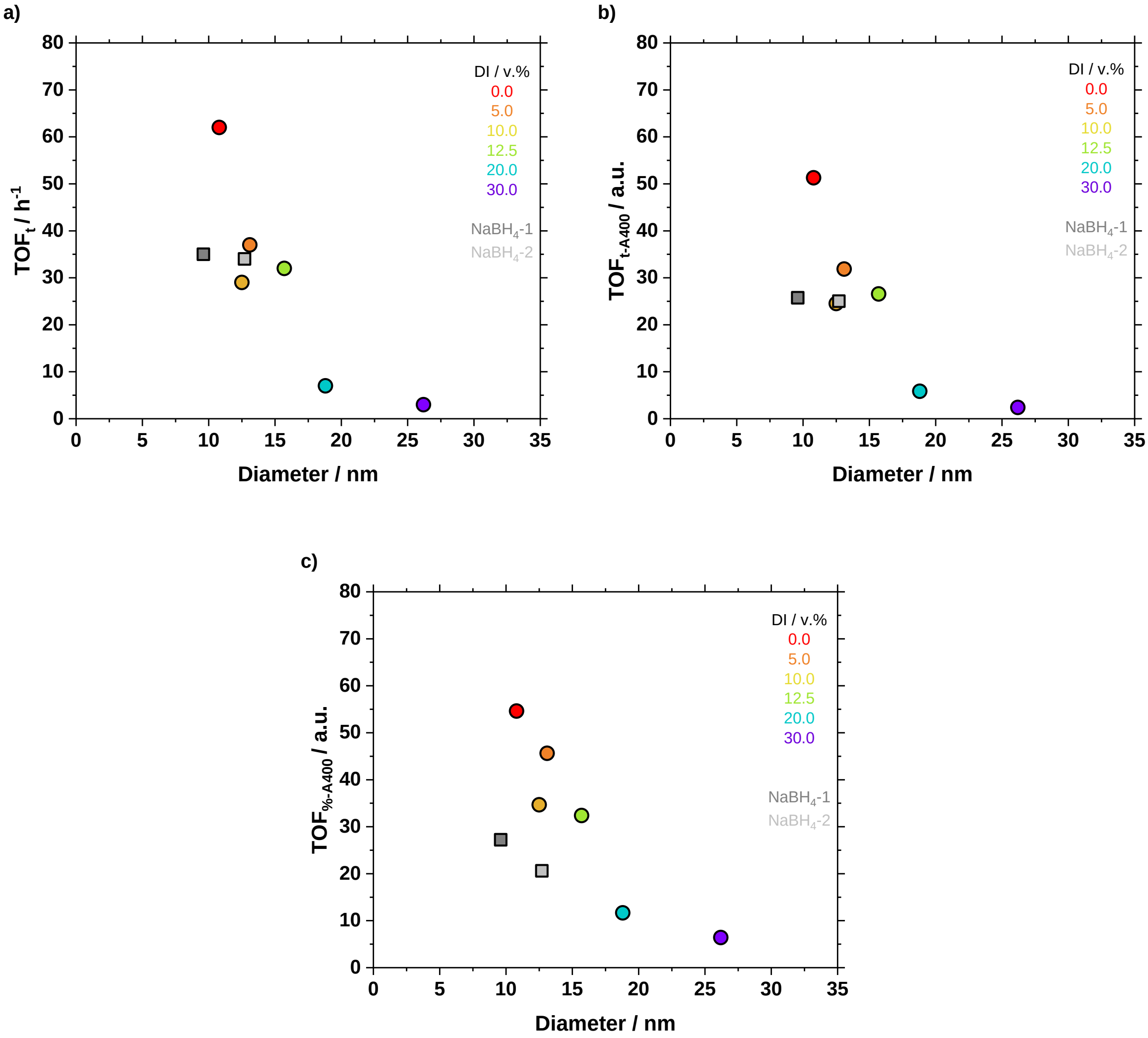

Figure S17. (a) TOF_t, (b) $TOF_{t\text{-}A400}$, (f) $TOF_{\%}$ and (c) $TOF_{\%\text{-}A400}$ as a function of the NP diameter for Au NPs prepared using different amounts of DI water or $NaBH_4$, as indicated. In all cases the molar ratio Au/4-NP was 5%. The data relate to **Figure 3** in the manuscript.

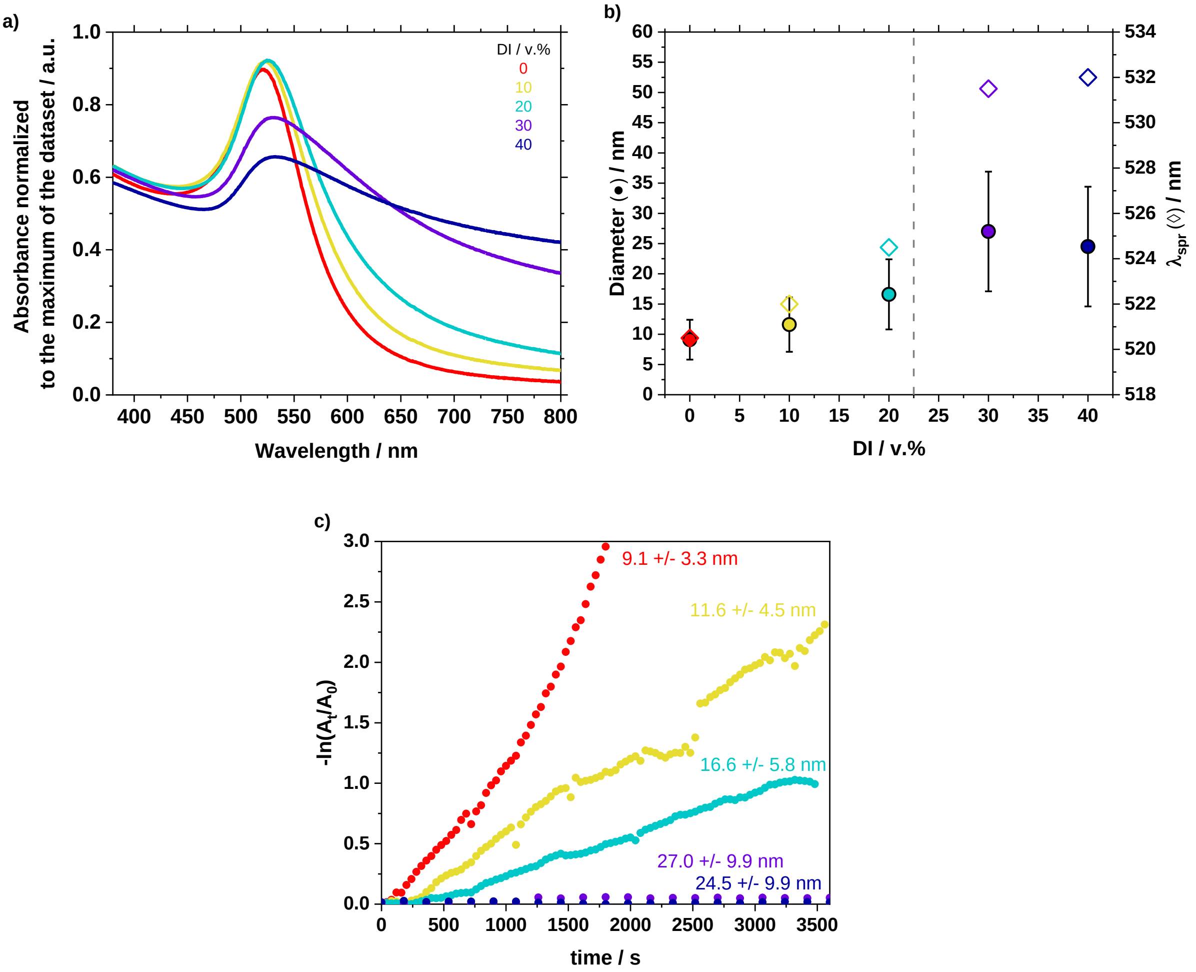
a)
Absorbance normalized to the maximum of the dataset / a.u.
Wavelength / nm
DI / v.%
0
10
20
30
40
b)
Diameter (●) / nm
λ_{spr} (◊) / nm
DI / v.%
c)
$-\ln(A_t/A_0)$
time / s
9.1 +/- 3.3 nm
11.6 +/- 4.5 nm
16.6 +/- 5.8 nm
27.0 +/- 9.9 nm
24.5 +/- 9.9 nm

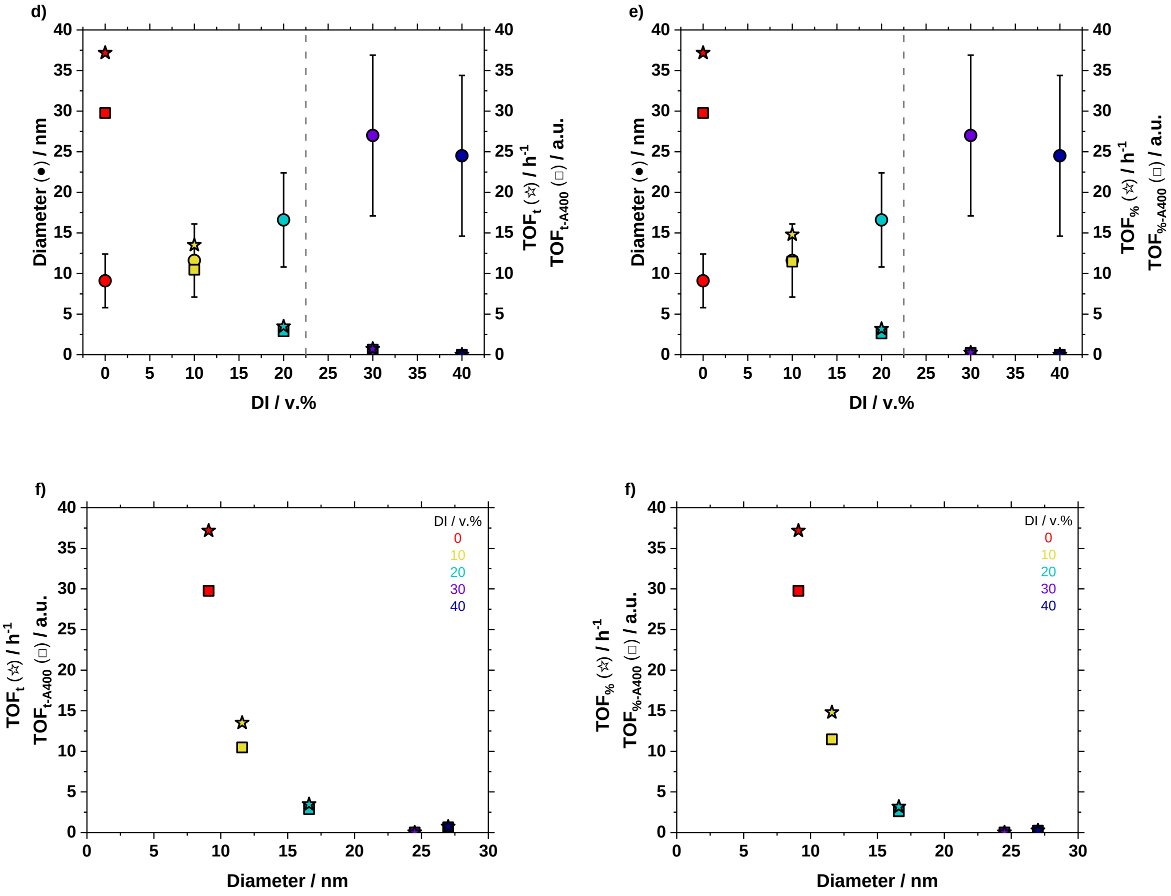

Figure S18. (a) UV-vis spectra of the Au NPs considered for the 4-NP reduction, obtained with different amounts of DI water, as indicated. High purity ethanol ($E_{98\%}$) was used as stock solution of ethanol for all experiments at a final content of 20 v.% for a total of 80 v.% water (DI+mQ). 0.5 mM $HAuCl_4$ and 2 mM NaOH were used in all cases. (b) Diameter and λ_{spr} values for the related samples. (c) -ln(A_t/A_0) as a function of time for the 4-NP reduction for different samples, as indicated. (d) Diameter, TOF_t, and $TOF_{t\text{-}A400}$, and (e) diameter $TOF_{\%}$ and $TOF_{\%\text{-}A400}$ as a function of DI water content. (f) TOF_t, and $TOF_{t\text{-}A400}$, and (g) $TOF_{\%}$ and $TOF_{\%\text{-}A400}$ as a function of Au NP size. In all cases the molar ratio Au/4-NP was 5%.

The results show a decrease in TOF as the NP size increases, which is expected from the lower surface area of the Au NPs. Note that presence of alcohol has been reported to decrease the activity of the Au NPs for the 4-NP reduction. It is shown here that residual ethanol is not an issue to obtain active Au NPs. This is especially clear when comparing the TOF obtained for the Au NPs obtained here compared to Au NPs prepared using $NaBH_4$.

Table S5. Overview of the NP typical size retrieved from STEM analysis and catalytic activity for 4-NP reduction. See **section S1** for further details and metrics.

A) Data corresponding to Figure S15.

Molar ratio Au/4-NP %	**Reducing agent and grade**	**DI** v.%	**Size** nm	**N**	**General shape**	**A$_{400}$**	**Final conversion reached** %	**Time to reach final conversion** s	**TOF$_{\%}$** h^{-1}	**TOF$_{\%\text{-A400}}$** a.u.	**Conversion reached at 960 s** %	**TOF$_{t}$** h^{-1}	**TOF$_{t\text{-A400}}$** a.u.
1.0	E$_{70\%}$	0.0	10.8 ± 3.4	201	Spherical	1.21	7	6000	4	3	1	3	2
2.5							65	2720	34	28	20	30	25
5.0							95	1040	66	55	82	62	51

B) Data corresponding to Figure S16. The molar ratio Au/4-NP was 5%.

Reducing agent and grade	**DI** v.%	**Size** nm	**N**	**General shape**	**A$_{400}$**	**Final conversion reached** %	**Time to reach final conversion** s	**TOF$_{\%}$** h^{-1}	**TOF$_{\%\text{-A400}}$** a.u.	**Conversion reached at 960 s** %	**TOF$_{t}$** h^{-1}	**TOF$_{t\text{-A400}}$** a.u.
E$_{70\%}$	0.0	10.8 ± 3.4	201	Spherical	1.21	95	1040	66	55	82	62	51
E$_{70\%}$	5.0	13.1 ± 5.3	158	Spherical	1.12	95	1280	53	46	49	37	32
E$_{70\%}$	10.0	12.5 ± 5.0	150	Spherical	1.18	95	1680	41	35	38	29	25
E$_{70\%}$	12.5	15.7 ± 5.0	175	Spherical	1.20	95	1740	39	32	42	32	27
E$_{70\%}$	20.0	18.8 ± 7.1	106	Spherical	1.20	39	1980	14	12	9	7	6
E$_{70\%}$	30.0	26.2 ± 8.6	118	Some not well defined shapes	1.25	14	1260	8	6	10	3	2
$NaBH_4$-1	0.0	9.6 ± 2.5	158	Spherical	1.36	95	1840	37	27	47	35	26
$NaBH_4$-2	0.0	12.7 ± 3.8	161	Spherical	1.36	95	2460	28	21	45	34	25
$HAuCl_4$	0.0	-	-	-	-	25	6600	3	3	6	4	4

C) Data corresponding to Figure S17. The molar ratio Au/4-NP was 5%.

Ethanol and grade	**DI** v.%	**Size** nm	**N**	**General shape**	A_{400}	**Final conversion reached** %	**Time to reach final conversion** s	$\text{TOF}_{\%}$ h^{-1}	$\text{TOF}_{\%\text{-}A400}$ a.u.	**Conversion reached at 960 s** %	TOF_{t} h^{-1}	$\text{TOF}_{t\text{-}A400}$ a.u.
$E_{70\%}$	0.0	10.8 ± 3.4	201	Spherical	1.21	89 ± 10	1133 ± 234	59 ± 14	49 ± 12	74 ± 26	55 ± 16	46 ± 13
$E_{70\%}$	5.0	13.1 ± 5.3	158	Spherical	1.12	83 ± 11	1307 ± 162	46 ± 6	40 ± 5	47 ± 6	35 ± 3	30 ± 3
$E_{70\%}$	10.0	12.5 ± 5.0	150	Spherical	1.18	81 ± 24	1540 ± 524	44 ± 21	37 ± 18	54 ± 36	40 ± 22	34 ± 19
$E_{70\%}$	12.5	15.7 ± 5.0	175	Spherical	1.20	69 ± 46	2413 ± 1656	33 ± 23	27 ± 19	39 ± 32	29 ± 20	24 ± 17
$E_{70\%}$	20.0	18.8 ± 7.1	106	Spherical	1.20	61 ± 38	2115 ± 1405	33 ± 25	27 ± 21	31 ± 34	23 ± 22	19 ± 18
$E_{70\%}$	30.0	26.2 ± 8.6	118	Some not well defined shapes	1.25	10 ± 4	2295 ± 1267	4 ± 3	3 ± 2	5 ± 3	4 ± 2	3 ± 2

D) Data corresponding to Figure S18. The molar ratio Au/4-NP was 5%.

Ethanol grade	**DI** v.%	**Size** nm	**N**	**General shape**	A_{400}	**Final conversion reached** %	**Time to reach final conversion** s	$\text{TOF}_{\%}$ h^{-1}	$\text{TOF}_{\%\text{-}A400}$ a.u.	**Conversion reached at 1840 s** %	TOF_{t} h^{-1}	$\text{TOF}_{t\text{-}A400}$ a.u.
$E_{98\%}$	0	9.1 ± 3.3	212	Spherical	1.25	95.00	1840	37	30	95	37	30
$E_{98\%}$	10	11.6 ± 4.5	112	Spherical	1.35	73.15	3560	15	11	35	14	10
$E_{98\%}$	20	16.6 ± 5.8	112	Spherical	1.21	14.25	3240	3	3	9	3	3
$E_{98\%}$	30	27.0 ± 9.9	107	Some not well defined shapes	1.12	1.81	5520	0	0	2	1	1
$E_{98\%}$	40.0	24.5 ± 9.9	152	Less well defined shapes	1.05	0	-	0	0	-	0	0

In the literature, a wide range of protocols,[31,34-36] setups (e.g. volumes), concentrations of chemicals, Au NP synthesis, sizes and loadings, supports, etc., are used.[22,31,34-39] The k_{app} values and TOF values obtained here are in the range reported in the literature typically between 0.000073 s^{-1} and 0.187 s^{-1} for k_{app} and 77 h^{-1} and 20561 h^{-1} for TOFs.[22,40-42] k_{app} values commonly cluster around $1 \cdot 10^{-3}$-$5 \cdot 10^{-3}$ s^{-1},[22,31,36,37,43] which aligns well with our results. TOF values vary significantly across the literature, largely due to differences in how researchers define and calculate it. This makes a direct comparison challenging, hence the preference here to use samples $NaBH_4$-1 and $NaBH_4$-2 to benchmark the activity of the SF Au NPs.

12- References

1 Quinson, J. *et al.* Surfactant-free colloidal syntheses of gold-based nanomaterials in alkaline water and mono-alcohol mixtures. *Chemistry of Materials* 35, 2173–2190 (**2023**). https://doi.org/10.1021/acs.chemmater.3c00090

2 Quinson, J. On the Importance of Fresh Stock Solutions for Surfactant-Free Colloidal Syntheses of Gold Nanoparticles in Alkaline Alcohol and Water Mixtures. *Inorganics* 11, 140 (**2023**). https://doi.org/10.3390/inorganics11040140

3 De Souza, C. D., Nogueira, B. R. & Rostelato, M. Review of the methodologies used in the synthesis gold nanoparticles by chemical reduction. *Journal of Alloys and Compounds* 798, 714-740 (**2019**). https://doi.org/10.1016/j.jallcom.2019.05.153

4 Quinson, J. Influence of the alcohol and water grades on surfactant-free colloidal syntheses of gold nanoparticles in alkaline water-alcohol mixtures. *Gold Bulletin* 57, 27-31 **(2024**). https://doi.org/10.1007/s13404-024-00345-7

5 Rasmussen, D. R., Lock, N. & Quinson, J. Lights on the synthesis of surfactant-free colloidal gold nanoparticles in alkaline mixtures of alcohols and water. *ChemSusChem* 18, e202400763 (**2025**). https://doi.org/10.1002/cssc.202400763

6 Deraedt, C. *et al.* Sodium borohydride stabilizes very active gold nanoparticle catalysts. *Chemical Communications* 50, 14194-14196 (**2014**). https://doi.org/10.1039/c4cc05946h

7 Freese, T., Elzinga, N., Heinemann, M., Lerch, M. M. & Feringa, B. L. The relevance of sustainable laboratory practices. *RSC Sustainability* 2, 1300-1336 (**2024**). https://doi.org/10.1039/D4SU00056K

8 Hutchison, J. E. The Road to Sustainable Nanotechnology: Challenges, Progress and Opportunities. *ACS Sustainable Chemistry & Engineering* 4, 5907-5914 (**2016**). https://doi.org/10.1021/acssuschemeng.6b02121

9 Gilbertson, L. M., Zimmerman, J. B., Plata, D. L., Hutchison, J. E. & Anastas, P. T. Designing nanomaterials to maximize performance and minimize undesirable implications guided by the Principles of Green Chemistry. *Chemical Society Reviews* 44, 5758-5777 (**2015**). https://doi.org/10.1039/c4cs00445k

10 Duan, H. H., Wang, D. S. & Li, Y. D. Green chemistry for nanoparticle synthesis. *Chemical Society Reviews* 44, 5778-5792 (**2015**).

11 Wuithschick, M. *et al.* Turkevich in New Robes: Key Questions Answered for the Most Common Gold Nanoparticle Synthesis. *ACS Nano* 9, 7052-7071 (**2015**). https://doi.org/10.1021/acsnano.5b01579

12 Liz-Marzan, L. M., Kagan, C. R. & Millstone, J. E. Reproducibility in Nanocrystal Synthesis? Watch Out for Impurities! *ACS Nano* 14, 6359-6361 (**2020**). https://doi.org/10.1021/acsnano.0c04709

13 Oestreicher, V., Garcia, C. S., Soler-Illia, G. & Angelome, P. C. Gold Recycling at Laboratory Scale: From Nanowaste to Nanospheres. *ChemSusChem* 12, 4882-4888 (**2019**). https://doi.org/10.1002/cssc.20190148

14 Mourdikoudis, S., Pallares, R. M. & Thanh, N. T. K. Characterization techniques for nanoparticles: comparison and complementarity upon studying nanoparticle properties. *Nanoscale* 10, 12871-12934 (**2018**). https://doi.org/10.1039/c8nr02278j

15 Villa, A. *et al.* Characterisation of gold catalysts. *Chemical Society Reviews* 45, 4953-4994 (**2016**). https://doi.org/10.1039/c5cs00350d

16 Hendel, T. *et al.* In Situ Determination of Colloidal Gold Concentrations with UV-Vis Spectroscopy: Limitations and Perspectives. *Analytical Chemistry* 86, 11115-11124 (**2014**). https://doi.org/10.1021/ac502053s

17 Amendola, V. & Meneghetti, M. Size Evaluation of Gold Nanoparticles by UV-vis Spectroscopy. *Journal of Physical Chemistry C* 113, 4277-4285 (**2009**). https://doi.org/10.1021/jp8082425

18 Haiss, W., Thanh, N. T. K., Aveyard, J. & Fernig, D. G. Determination of size and concentration of gold nanoparticles from UV-Vis spectra. *Analytical Chemistry* 79, 4215-4221 (**2007**). https://doi.org/10.1021/ac0702084

19 Panariello, L., Radhakrishnan, A. N. P., Papakonstantinou, I., Parkin, I. P. & Gavriilidis, A. Particle Size Evolution during the Synthesis of Gold Nanoparticles Using In Situ Time-Resolved UV-Vis Spectroscopy: An Experimental and Theoretical Study Unravelling the Effect of Adsorbed Gold Precursor Species. *Journal of Physical Chemistry C* 124, 27662-27672 (**2020**). https://doi.org/10.1021/acs.jpcc.0c07405

20 Neal, R., Inoue, Y., Hughes, R. & Neretina, S. Catalytic Reduction of 4-Nitrophenol by Gold Catalysts: The Influence of Borohydride Concentration on the Induction Time. *Journal of Physical Chemistry C* 123, 12894-12901 (**2019**). https://doi.org/10.1021/acs.jpcc.9b02396

21 Pradhan, N., Pal, A. & Pal, T. Catalytic reduction of aromatic nitro compounds by coinage metal nanoparticles. *Langmuir* 17, 1800-1802 (**2001**).

22 Larm, N. E., Bhawawet, N., Thon, J. A. & Baker, G. A. Best practices for reporting nanocatalytic performance: lessons learned from nitroarene reduction as a model reaction. *New Journal of Chemistry* 43, 17932-17936 (**2019**). https://doi.org/10.1039/c9nj01745c

23 Merk, V. *et al.* In Situ Non-DLVO Stabilization of Surfactant-Free, Plasmonic Gold Nanoparticles: Effect of Hofmeister's Anions. *Langmuir* 30, 4213-4222 (**2014**). https://doi.org/10.1021/la404556a

24 Ye, Y. J., Lv, M. X., Zhang, X. Y. & Zhang, Y. X. Colorimetric determination of copper(II) ions using gold nanoparticles as a probe. *RSC Advances* 5, 102311-102317 (**2015**). https://doi.org/10.1039/c5ra20381c

25 Agarwal, S. *et al.* Citrate-capped gold nanoparticles for the label-free detection of ubiquitin C-terminal hydrolase-1. *Analyst* 140, 1166-1173 (**2015**). https://doi.org/10.1039/c4an01935k

26 Parveen, R., Ullah, S., Sgarbi, R. & Tremiliosi, G. One-pot ligand-free synthesis of gold nanoparticles: The role of glycerol as reducing-cum-stabilizing agent. *Colloids and Surfaces a-Physicochemical and Engineering Aspects* 565, 162-171 (**2019**). https://doi.org/10.1016/j.colsurfa.2019.01.005

27 Rasmussen, D. R., Nielsen, M. F. & Quinson, J. Room Temperature Surfactant-Free Synthesis of Gold Nanoparticles in Alkaline Ethylene Glycol. *Chemistry* 5, 900-911 (**2023**). https://doi.org/10.3390/chemistry5020061

28 Quinson, J., Kunz, S. & Arenz, M. Beyond Active Site Design: A Surfactant-Free Toolbox Approach for Optimized Supported Nanoparticle Catalysts. *ChemCatChem* 13, 1692-1705 (**2021**). ttps://doi.org/10.1002/cctc.202001858

29 Quinson, J., Nielsen, T. M., Escudero-Escribano, M. & Jensen, K. M. Ø. Room temperature syntheses of surfactant-free colloidal gold nanoparticles: the benefits of mono-alcohols over polyols as reducing agents for electrocatalysis. *Colloids and Surfaces A: Physicochemical and Engineering Aspects*, 675, 131853 (**2023**). https://doi.org/10.1016/j.colsurfa.2023.131853

30 Varga, M. & Quinson, J. Fewer, but better: on the benefits for surfactant-free colloidal syntheses of nanomaterials. *ChemistrySelect* 10, e202404819 (**2025**). https://doi.org/10.1002/slct.202404819

31 Teimouri, M. *et al.* Gold nanoparticles fabrication by plant extracts: synthesis, characterization, degradation of 4-nitrophenol from industrial wastewater, and insecticidal activity - A review. *Journal of Cleaner Production* 184, 740-753 (**2018**). https://doi.org/10.1016/j.jclepro.2018.02.268

32 Zhao, P., Feng, X., Huang, D., Yang, G. & Astruc, D. Basic concepts and recent advances in nitrophenol reduction by gold- and other transition metal nanoparticles. *Coordination Chemistry Reviews* 287, 114-136 (**2015**). https://doi.org/10.1016/j.ccr.2015.01.002

33 Mejía, Y. & Bogireddy, N. Reduction of 4-nitrophenol using green-fabricated metal nanoparticles. *RSC Advances* 12, 18661-18675 (**2022**). https://doi.org/10.1039/d2ra02663e

34 Gu, S. S. *et al.* Ligand-free Gold Nanoparticles as a Reference Material for Kinetic Modelling of Catalytic Reduction of 4-Nitrophenol. *Catalysis Letters* 145, 1105-1112 (**2015**). https://doi.org/10.1007/s10562-015-1514-7

35 Devi, H. S., Singh, N. R., Singh, H. P. & Singh, T. D. Facile synthesis of biogenic gold nanocatalyst for efficient degradation of organic pollutants. *Journal of Environmental Chemical Engineering* 3, 2042-2049 (**2015**). https://doi.org/10.1016/j.jece.2015.07.014

36 Neal, R. D., Hughes, R. A., Sapkota, P., Ptasinska, S. & Neretina, S. Effect of Nanoparticle Ligands on 4-Nitrophenol Reduction: Reaction Rate, Induction Time, and Ligand Desorption. *ACS Catalysis* 10, 10040-10050 (**2020**). https://doi.org/10.1021/acscatal.0c02759

37 Ansar, S. & Kitchens, C. Impact of Gold Nanoparticle Stabilizing Ligands on the Colloidal Catalytic Reduction of 4-Nitrophenol. *ACS Catalysis* 6, 5553-5560 (**2016**). https://doi.org/10.1021/acscatal.6b00635

38 Lin, C., Tao, K., Hua, D., Ma, Z. & Zhou, S. Size Effect of Gold Nanoparticles in Catalytic Reduction of p-Nitrophenol with $NaBH_4$. *Molecules* 18, 12609-12620 (**2013**). https://doi.org/10.3390/molecules181012609

39 Hu, C. *et al.* Rapid and facile synthesis of Au nanoparticle-decorated porous MOFs for the efficient reduction of 4-nitrophenol. *Separation and Purification technology* 300, 121801 (**2022**). https://doi.org/10.1016/j.seppur.2022.121801

40 Larm, N. E., Thon, J. A., Vazmitsel, Y., Atwood, J. L. & Baker, G. A. Borohydride stabilized gold-silver bimetallic nanocatalysts for highly efficient 4-nitrophenol reduction. *Nanoscale Advances* 1, 4665-4668 (**2019**). https://doi.org/10.1039/c9na00645a

41 Wunder, S., Lu, Y., Albrecht, M. & Ballauff, M. Catalytic Activity of Faceted Gold Nanoparticles Studied by a Model Reaction: Evidence for Substrate-Induced Surface Restructuring. *ACS Catalysis* 1, 908-916 (**2011**). https://doi.org/10.1021/cs200208a

42 Shanmugaraj, K., Bustamante, T., Torres, C. & Campos, C. Gold nanoparticles supported on mesostructured oxides for the enhanced catalytic reduction of 4-nitrophenol in water. *Catalysis Today* 388-389, 383-393 (**2022**). https://doi.org/10.1016/j.cattod.2020.05.051

43 Molina, H. *et al.* Carbon Supported Gold Nanoparticles for the Catalytic Reduction of 4-Nitrophenol. *Frontiers in Chemistry* 7, 548 (**2019**). https://doi.org/10.3389/fchem.2019.00548